Article

Developmental Cell

# Organ-specific COP1 control of BES1 stability adjusts plant growth patterns under shade or warmth

## Graphical abstract

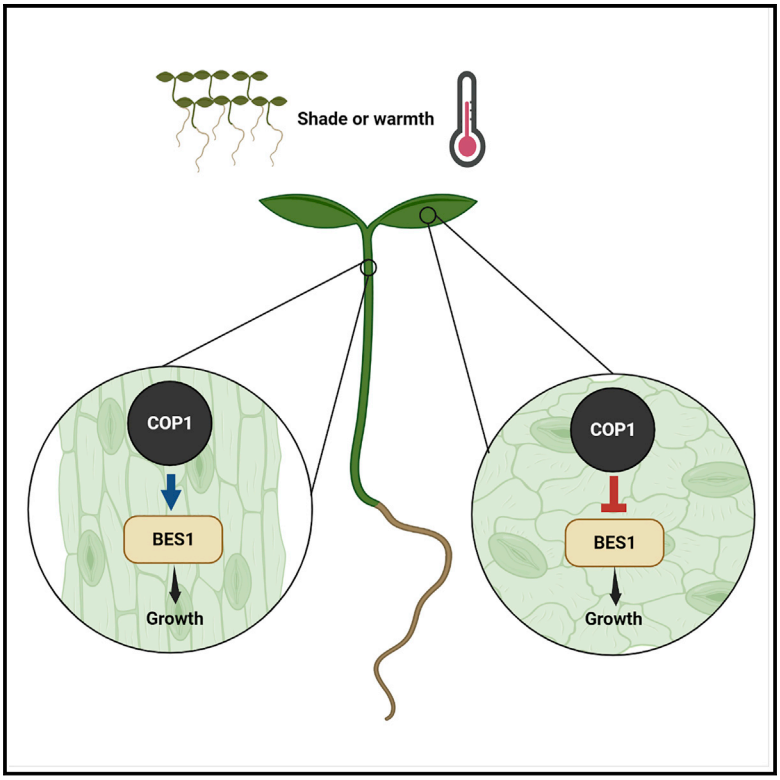


## Authors

Cecilia Costigliolo Rojas, Luciana Bianchimano, Jeonghwa Oh, ..., David Alabadi, Matias D. Zurbriggen, Jorge J. Casal

## Correspondence

casal@ifeva.edu.ar

## In brief

To face environmental challenges, plants have to adjust the growth of their organs selectively. Costigliolo-Rojas et al. show that the mechanisms of growth regulation involve the same molecular components differentially connected in the cotyledons and hypocotyl.

## Highlights

- Shade or warmth reduces BES1 abundance to restrict cotyledon expansion
- Under shade or warmth, COP1 physically interacts with BES1
- COP1 targets BES1 to degradation in the cotyledons, but not in the hypocotyl
- Under shade or warmth, PIF4 reduces *BES1* expression

Costigliolo Rojas et al., 2022, Developmental Cell *57*, 1–17
August 22, 2022 
https://doi.org/10.1016/j.devcel.2022.07.003

CellPress

Developmental Cell

CellPress

Article

# Organ-specific COP1 control of BES1 stability adjusts plant growth patterns under shade or warmth

Cecilia Costigliolo Rojas,[1] Luciana Bianchimano,[1] Jeonghwa Oh,[2] Sofía Romero Montepaone,[3] Dana Tarkowská,[4] Eugenio G. Minguet,[5] Jonas Schön,[3] Mariano García Hourquet,[1] Timo Flugel,[1] Miguel A. Blázquez,[5] Giltsu Choi,[2] Miroslav Strnad,[4] Santiago Mora-García,[1] David Alabadi,[5] Matias D. Zurbriggen,[3] and Jorge J. Casal[1,6,7,*]

[1]Fundación Instituto Leloir, Instituto de Investigaciones Bioquímicas de Buenos Aires, Consejo Nacional de Investigaciones Científicas y Técnicas, 1405 Buenos Aires, Argentina

[2]Department of Biological Sciences, Korea Advanced Institute of Science and Technology, Daejeon 34141, South Korea

[3]Institute of Synthetic Biology and Cluster of Excellence in Plant Sciences, University of Düsseldorf, 40225 Düsseldorf, Germany

[4]Laboratory of Growth Regulators, Palacký University and Institute of Experimental Botany, Czech Academy of Sciences, Olomouc, Czech Republic

[5]Instituto de Biología Molecular y Celular de Plantas, Consejo Superior de Investigaciones Científicas, Universidad Politécnica de Valencia, 46022 Valencia, Spain

[6]Instituto de Investigaciones Fisiológicas y Ecológicas Vinculadas a la Agricultura, Facultad de Agronomía, Universidad de Buenos Aires, Consejo Nacional de Investigaciones Científicas y Técnicas, 1417 Buenos Aires, Argentina

[7]Lead contact

*Correspondence: casal@ifeva.edu.ar

https://doi.org/10.1016/j.devcel.2022.07.003

## SUMMARY

Under adverse conditions such as shade or elevated temperatures, cotyledon expansion is reduced and hypocotyl growth is promoted to optimize plant architecture. The mechanisms underlying the repression of cotyledon cell expansion remain unknown. Here, we report that the nuclear abundance of the BES1 transcription factor decreased in the cotyledons and increased in the hypocotyl in *Arabidopsis thaliana* under shade or warmth. Brassinosteroid levels did not follow the same trend. PIF4 and COP1 increased their nuclear abundance in both organs under shade or warmth. PIF4 directly bound the *BES1* promoter to enhance its activity but indirectly reduced *BES1* expression. COP1 physically interacted with the BES1 protein, promoting its proteasome degradation in the cotyledons. COP1 had the opposite effect in the hypocotyl, demonstrating organ-specific regulatory networks. Our work indicates that shade or warmth reduces BES1 activity by transcriptional and post-translational regulation to inhibit cotyledon cell expansion.

## INTRODUCTION

One of the most conspicuous changes induced in young dicotyledonous seedlings both by the drop of the light input observed under shade (Ballaré and Pierik, 2017; Casal, 2013) and by warm (non-stressful) temperatures (Casal and Balasubramanian, 2019; Quint et al., 2016) is the promotion of hypocotyl growth. Conversely, shade cues (Josse et al., 2011; Li et al., 2012; Procko et al., 2014) and warmth (Hahm et al., 2020) reduce cotyledon expansion. This organ-specific effects adjust plant morphogenesis to the prevailing conditions of the environment. Similar effects occur in the stem and leaves as plants progress in their life cycle (Roig-Villanova and Martínez-García, 2016). However, in contrast to the growth of post-embryonic stems and leaves, which depends on cell division as well as cell expansion, the growth of the hypocotyl (Gendreau et al., 1997) and cotyledons (Tsukaya et al., 1994) depends exclusively on cell expansion, offering excellent systems to specifically focus on this process. The mechanisms involved in the responses of foliage cell expansion to shade and warmth remain poorly understood.

The cues perceived by environmental sensors modify the activity of transcriptional regulators that in turn affect the signaling status of growth hormones. Among these sensors is phytochrome B (phyB), and both shade (Sellaro et al., 2019) and warm temperatures (Jung et al., 2016; Legris et al., 2016) reduce the activity of phyB. phyB represses the activity of the bHLH transcription factors PHYTOCHROME-INTERACTING FACTORs (PIFs) such as PIF4, PIF5, and PIF7 (Huang et al., 2018; Park et al., 2018; Pham et al., 2018a), and the activity of the E3 ligase CONSTITUTIVELY PHOTOMORPHOGENIC 1 (COP1) (Lau and Deng, 2012; Sheerin et al., 2015). PIF4, PIF5 (Koini et al., 2009; Legris et al., 2017; Lorrain et al., 2008), PIF7 (Chung et al., 2020; Fiorucci et al., 2020; Huang et al., 2018; Li et al., 2012), and COP1 (Pacín et al., 2016; Park et al., 2017) accumulate in the nucleus in response to the reduced phyB

Please cite this article in press as: Costigliolo Rojas et al., Organ-specific COP1 control of BES1 stability adjusts plant growth patterns under shade or warmth, Developmental Cell (2022), https://doi.org/10.1016/j.devcel.2022.07.003



activity caused by shade or warmth. Under these conditions, COP1 induces the degradation of negative regulators of PIFs (Blanco-Touriñán et al., 2020; Pacín et al., 2016; Park et al., 2017).

Auxin, gibberellins, and brassinosteroid signaling play a fundamental role in hypocotyl-growth responses to shade and warmth (Ballaré and Pierik, 2017; Casal, 2013; Casal and Balasubramanian, 2019; Quint et al., 2016). Both environmental cues rapidly increase the synthesis of auxin in the cotyledons—thanks to the enhanced activity of mainly PIF4, PIF5, and PIF7, which bind the promoters of auxin synthesis genes (Franklin et al., 2011; Hornitschek et al., 2012; Li et al., 2012; Sun et al., 2012). Auxin travels to the hypocotyl to promote growth (Bellstaedt et al., 2019; Procko et al., 2014). Later on, the levels of auxin return to the pre-stimulation values, but the system is more sensitive to residual auxin (Pucciariello et al., 2018). Gibberellins induce the degradation of DELLA (aspartic acid–glutamic acid–leucine–leucine–alanine) motif proteins such as REPRESSOR OF *ga1-3* (RGA) (Sun, 2011). DELLAs are negative regulators of transcription factors like PIFs (Feng et al., 2008; De Lucas et al., 2008) and BRASSINAZOLE (BRZ)-RESISTANT 1 (BZR1) (Bai et al., 2012; Gallego-Bartolomé et al., 2012), which are involved in the promotion of growth. Shade and warmth increase gibberellin levels, but these changes are relatively slow (Blanco-Touriñán et al., 2020; Bou-Torrent et al., 2014). In the hypocotyl, rapid de-stabilization of DELLA proteins by shade and warmth results from COP1-mediated targeting to degradation (Blanco-Touriñán et al., 2020). Warm temperatures promote the expression of brassinosteroid biosynthetic genes during the night (Purlyte et al., 2018), whereas simulated shade does not increase the level of brassinosteroids (Bou-Torrent et al., 2014; Kurepin et al., 2012). Shade can enhance the expression of the brassinosteroid receptor *BRASSINOSTEROID INSENSITIVE 1* (*BRI1*) gene (Roig-Villanova et al., 2006; Sorin et al., 2009), but warmth reduces BRI1 abundance in the root (Martins et al., 2017). BZR1 and BR-INSENSITIVE1-EMS-SUPPRESSOR 1 (BES1) are two transcription factors involved in the responses to brassinosteroids (Nolan et al., 2020). Shade can increase the abundance of the de-phosphorylated form of BES1 (Hayes et al., 2019), and warmth has the same effect during the night (Purlyte et al., 2018) but not under continuous light (Stavang et al., 2009). Warmth can also increase the nuclear abundance of BZR1 (Ibañez et al., 2018). As summarized recently, we still need to better understand how brassinosteroids contribute mechanistically to the overall growth program of plants, particularly under shade or warmth (Nolan et al., 2020).

phyB promotes (Neff and Van Volkenburgh, 1994), whereas PIF4 (Huq and Quail, 2002) and COP1 (Deng et al., 1991) inhibit, cotyledon expansion. Taking into account their dynamics under shade or warmth, phyB, PIF4, and COP1 are likely to participate in the repression imposed by these environmental cues. However, the downstream hormone-related mechanisms are not known. As described above, shade and warmth rapidly enhance auxin levels in the cotyledons (Bellstaedt et al., 2019; Procko et al., 2014). Although exogenous auxin can reduce cotyledon expansion (Enders et al., 2017), endogenous auxin causes the opposite effect (Lewis et al., 2009; Strader et al., 2010). Therefore, it is not clear whether changes in auxin mediate the inhibition of cotyledon expansion by shade and warmth. Gibberellins promote cotyledon expansion, whereas DELLAs, the negative regulators of gibberellin signaling, have the opposite effect (Josse et al., 2011). In seedlings grown for several days under red light plus far-red light, RGA is more abundant than in the red-light controls and the *phyB* mutant has high RGA even under red light (Josse et al., 2011). Since increased proportion of far-red light is a key component of the shade cue that lowers phyB activity, gibberellins could participate in cotyledon expansion responses to shade. Mutants deficient in brassinosteroid have large cotyledons in darkness (Chory et al., 1991), and exogenous brassinosteroid reduces cotyledon size in light-grown seedlings (Beuchat et al., 2010); however, mutants deficient in brassinosteroid catabolism also have large cotyledons in the light (Turk et al., 2005).

In crops, light interception for photosynthesis and water loss through transpiration depend on the area of the foliage. Cotyledon expansion is a chief component of early seedling vigor, an agronomic trait that affects these physiological processes during seedling establishment. Furthermore, cotyledon expansion offers a model for cell expansion in post-embryonic leaves. Given the current scenario of global warming and the trend to increase sowing densities in crops (which results in enhanced competition for light), it is important to understand the mechanisms of cotyledon cell expansion responses to shade and warmth. Here, we show that these mechanisms involve phyB, COP1, PIF4, and BES1.

## RESULTS

### Gibberellins, auxin, and brassinosteroid signaling in the response of cotyledon expansion to shade and warmth

We investigated the role of gibberellins, auxin, and brassinosteroid signaling in epidermal cells in the control of cotyledon expansion by shade and warmth. We focused on this tissue because the epidermis plays a major role in the control of shoot growth in *A. thaliana* seedlings (Savaldi-Goldstein et al., 2007).

Gibberellins promote cotyledon expansion by lowering DELLA (Josse et al., 2011); we therefore tested the hypothesis that shade and/or warmth reduce gibberellin and increase DELLA in epidermal cells to lower cotyledon expansion rates. A mutant lacking RGA and other DELLA proteins showed enhanced cotyledon expansion under shade or warmth (Figure S1A), suggesting that, if it occurred, an increase of RGA levels would reduce growth under those conditions. However, *pRGA:RGA-GFP*-driven fluorescence remained unaffected 4 or 8 h after transfer from control conditions to shade or warmth (Figure 1A). The nuclear fluorescence driven by *pRGA:RGA-GFP* plummeted in response to exogenous gibberellin and increased in response to the gibberellin synthesis inhibitor Paclobutrazol, indicating that it is a sensitive proxy for gibberellin signaling status (Figure 1A, see also Silverstone et al., 2001). Therefore, although the gibberellin-DELLA pathway is essential for wild-type (WT) cotyledon expansion responses, its status does not change in epidermal cells in response to shade or warmth, providing evidence against the above hypothesis.

Shade and warmth increase auxin signaling in the cotyledons (Franklin et al., 2011; Hornitschek et al., 2012; Li et al., 2012; Sun et al., 2012), as reflected by the increased nuclear fluorescence driven by the marker of auxin-induced transcriptional

Please cite this article in press as: Costigliolo Rojas et al., Organ-specific COP1 control of BES1 stability adjusts plant growth patterns under shade or warmth, Developmental Cell (2022), https://doi.org/10.1016/j.devcel.2022.07.003



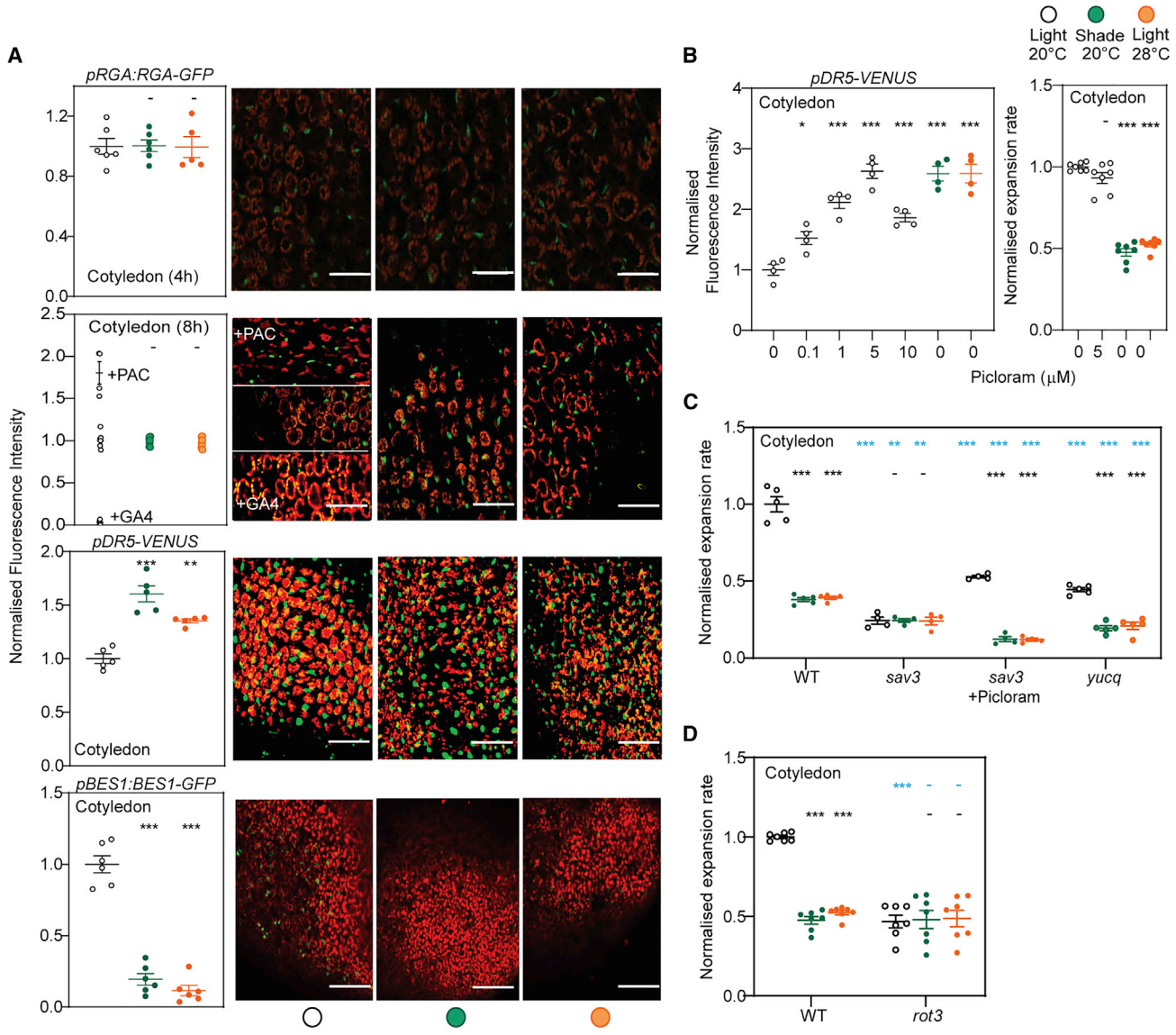


**Figure 1. Brassinosteroid, gibberellin, and auxin signaling in the response of cotyledon expansion to shade and warmth**

(A) Markers of gibberellins (*pRGA:RGA-GFP*), auxin (*pDR5:VENUS*), and brassinosteroid (*pBES1:BES1-GFP*) signaling in the cotyledons, under control conditions (light at 20°C) and 4 h (or 8 h) after transfer to shade or warmth. Fluorescence driven by *pRGA:RGA-GFP* after addition of 5 μM paclobutrazol (+Paclo) or 3 μM gibberellin (+GA4) under control conditions is also included.

(B) A dose of the synthetic auxin picloram that enhances fluorescence driven by *pDR5:VENUS* to the same levels of shade or warmth (left) did not reduce cotyledon expansion as shade or warmth (right).

(C and D) Cotyledon expansion rate in the *sav3* and quintuple *yuc* (*yucq*) mutants impaired in auxin synthesis, the *sav3* supplemented with 5-μM picloram (C) and the *rot3* mutant impaired in brassinosteroid synthesis (D) during 9 h after transfer to shade or warmth. Data are means ± SE (standard error) and individual values of 4–7 replicate boxes of seedlings and representative confocal images (scale bars, 35 μm). The asterisks indicate the statistical significance of the differences between the treatments (shade, warmth, or picloram) and the control (light at 20°C) for the same genotype (black) and between the mutant and the wild type under the same condition (blue): *p < 0.05; **p < 0.01; ***p < 0.001; -, not significant.

Also see Figure S1.

activity *pDR5:VENUS* in these organs (Figure 1A). At high concentrations, auxin can inhibit cotyledon growth (Enders et al., 2017); we therefore tested the hypothesis that elevated auxin in epidermal cells mediates the cotyledon growth inhibition under shade or warmth. Adding 5 μM of the synthetic auxin Picloram increased the fluorescence driven by *pDR5:VENUS* in the epidermal cells of the cotyledons to levels similar to those induced by shade or warmth (Figure 1B). However, adding 5 μM of Picloram did not affect cotyledon expansion (Figure 1B), arguing against the above hypothesis. Of note, 5 μM of Picloram is a treatment typically used to promote hypocotyl growth (Savaldi-Goldstein et al., 2008). The auxin synthesis *yuc3 yuc5 yuc7 yuc8 yuc9* (*yucq*) and *sav3* mutants (Tao et al., 2008) showed reduced cotyledon expansion under control conditions

Please cite this article in press as: Costigliolo Rojas et al., Organ-specific COP1 control of BES1 stability adjusts plant growth patterns under shade or warmth, Developmental Cell (2022), https://doi.org/10.1016/j.devcel.2022.07.003



(Figure 1C), indicating that the low concentrations of auxin of these mutants limits the growth of their cotyledons. Shade or warmth reduced cotyledon expansion in the *yucq* mutant and the *sav3* mutant supplemented with Picloram (Figure 1C) despite their impaired auxin synthesis, arguing in favor of other mechanisms of control.

Nuclear fluorescence driven by *pBES1:BES1-GFP* increases with brassinosteroids (Yin et al., 2002) and decreased in the cotyledons in response to shade or warmth (Figure 1A). The *rot3* (Figure 1D) and *det2* (Figure S1A) mutants, deficient in brassinosteroid synthesis (Fujioka et al., 1997; Ohnishi et al., 2006), showed reduced cotyledon expansion, indicating that reduced signaling through this pathway could indeed reduce cotyledon growth. Although the results of this triage do not dismiss a role of changes in gibberellins or auxin in inner cotyledon tissues, they prompted us to focus on the mechanisms by which shade and warmth reduce nuclear BES1 in the cotyledons and its contribution to the growth inhibition.

## BES1 and BZR1 levels decrease in the cotyledons and increase in the hypocotyl under shade or warmth

Nuclear fluorescence driven by *pBES1:BES1-GFP* (Figure 2A) or *pBZR1:BZR1-GFP* (Figure 2B) decreased in the cotyledons and increased in the hypocotyl in response to shade or warmth. Consistently with the results of confocal microscopy, in isolated cotyledons of *A. thaliana*, shade and warmth reduced BES1 abundance, with a stronger effect on the phosphorylated form (Figure 2C). To compare cotyledon and hypocotyl patterns, we shifted to *B. napus*, which being genetically related to *A. thaliana* is more convenient for organ isolation due to its size (Procko et al., 2014), and showed similar growth responses (Figure S1B). Under shade or warmth, BES1 protein levels increased in the hypocotyl and decreased in the cotyledons without affecting the ratio between the de-phosphorylated and phosphorylated forms (Figure 2D).

Upon transfer from shade or warmth to control conditions, nuclear fluorescence driven by *pBES1:BES1-GFP* decreased in the hypocotyl and increased in the cotyledons, and the values measured 4 h after the shift reached or closely approached those corresponding to seedlings under control conditions at all times (i.e., 1; Figure S2C). These results indicate that shade and warmth reversibly affect nuclear BES1 in opposite directions in the cotyledons and hypocotyls.

## Brassinosteroid levels under shade or warmth

Warm temperature did not decrease the expression of selected brassinosteroid synthesis genes in the cotyledons (Figure S3B). We analyzed the levels of active brassinosteroids (brassinolide, epibrassinolide [EBL], and castasterone) and several precursors (norcastasterone, homocastasterone, dolichosterone, homodolichosterone, and typhasterol) in hypocotyl and cotyledon samples harvested separately. If organ-level changes in active brassinosteroids mediate BES1 responses via the canonical pathway, we would expect a direct relationship between both variables; i.e., shade and warmth should elevate hormone levels in the hypocotyl and reduce these levels in the cotyledons. Although we cannot rule out localized effects, which can be biologically meaningful (Michaud et al., 2017; Pantazopoulou et al., 2017; Procko et al., 2016), at the whole organ level, none of the active compounds followed this pattern in *A. thaliana* (Figure 3C). In *B. napus*, brassinolide and castasterone levels in the hypocotyl and EBL levels in cotyledons showed the expected pattern in seedlings transferred to warmth but not to shade (Figure S3D). Therefore, although changes in brassinosteroid levels could contribute to the observed BES1 dynamics in this species, they do not provide a consistent explanation of the observed patterns, particularly upon transfer to shade. Actually, some of the compounds responded to shade or warmth opposite to the direction predicted by the above hypothesis. These changes could be the consequence of the negative feedback of BES1 on the expression of brassinosteroid synthesis genes (He et al., 2005), yielding a negative, rather than a positive correlation between BES1 and brassinosteroids.

## Shade or warmth reduces the nuclear levels of BES1 even under conditions of impaired brassinosteroid synthesis or sensitivity

We used the brassinosteroid synthesis inhibitor BRZ to reduce the hormone to levels that render nuclear fluorescence driven by *pBES1:BES1-GFP* undetectable (Figure 3A). In the presence of this synthesis inhibitor, exogenous brassinolide restored BES1 nuclear levels and their decrease in response to shade or warmth (Figure 3A). These results indicate that BES1 levels can respond to shade and warmth in the absence of differential brassinosteroid synthesis induced by these cues.

Shade and warmth reduced nuclear fluorescence driven by *p35S:bes1-D-GFP* in the cotyledons (Figure 3B), and shade reduced the mutant protein present in *bes1-D* (Figure S2D). Since this protein responds poorly to brassinosteroids (Yin et al., 2002), the results indicate that shade and warmth can affect BES1 by mechanisms other than changes in brassinosteroid levels. Conversely, shade and warmth did not increase nuclear fluorescence driven by *p35S:bes1-D-GFP* in the hypocotyl (Figure 3B), supporting the occurrence of different molecular pathways in both organs.

## Wild-type responses of BES1 nuclear levels to shade or warmth require phyB, COP1, and PIF4

Since phyB promotes and PIF4 and COP1 inhibit cotyledon expansion (Deng et al., 1991; Huq and Quail, 2002; Neff and Van Volkenburgh, 1994), we investigated whether they affected the abundance of nuclear BES1. First of all, we confirmed that phyB, PIF4, and COP1 change in the cotyledons in response to shade and warmth in the same direction reported earlier for the hypocotyl, i.e., the size of the phyB nuclear bodies decreases and the nuclear abundance of COP1 and PIF4 increases in response to both cues (Blanco-Touriñán et al., 2020; Legris et al., 2016, 2017; Figures 4A–4C). Then, we introgressed the *pBES1:BES1-GFP* transgene into the *phyB*, *cop1*, and *pif4* mutant backgrounds. In the cotyledons of *phyB*, nuclear BES1 showed reduced levels under control conditions; i.e., showed a constitutive response to shade or warmth (Figure 4D). In the hypocotyl of *phyB*, the levels of nuclear BES1 failed to increase in response to shade or warmth (Figure 4D). In the *cop1* mutant, nuclear BES1 showed WT levels under control conditions in both organs (Figure 4E). In the hypocotyl of *cop1*, shade or warmth failed to increase nuclear BES1. In the cotyledons of *cop1*, shade or warmth failed to decrease nuclear BES1. In other words, the

Please cite this article in press as: Costigliolo Rojas et al., Organ-specific COP1 control of BES1 stability adjusts plant growth patterns under shade or warmth, Developmental Cell (2022), https://doi.org/10.1016/j.devcel.2022.07.003



CellPress

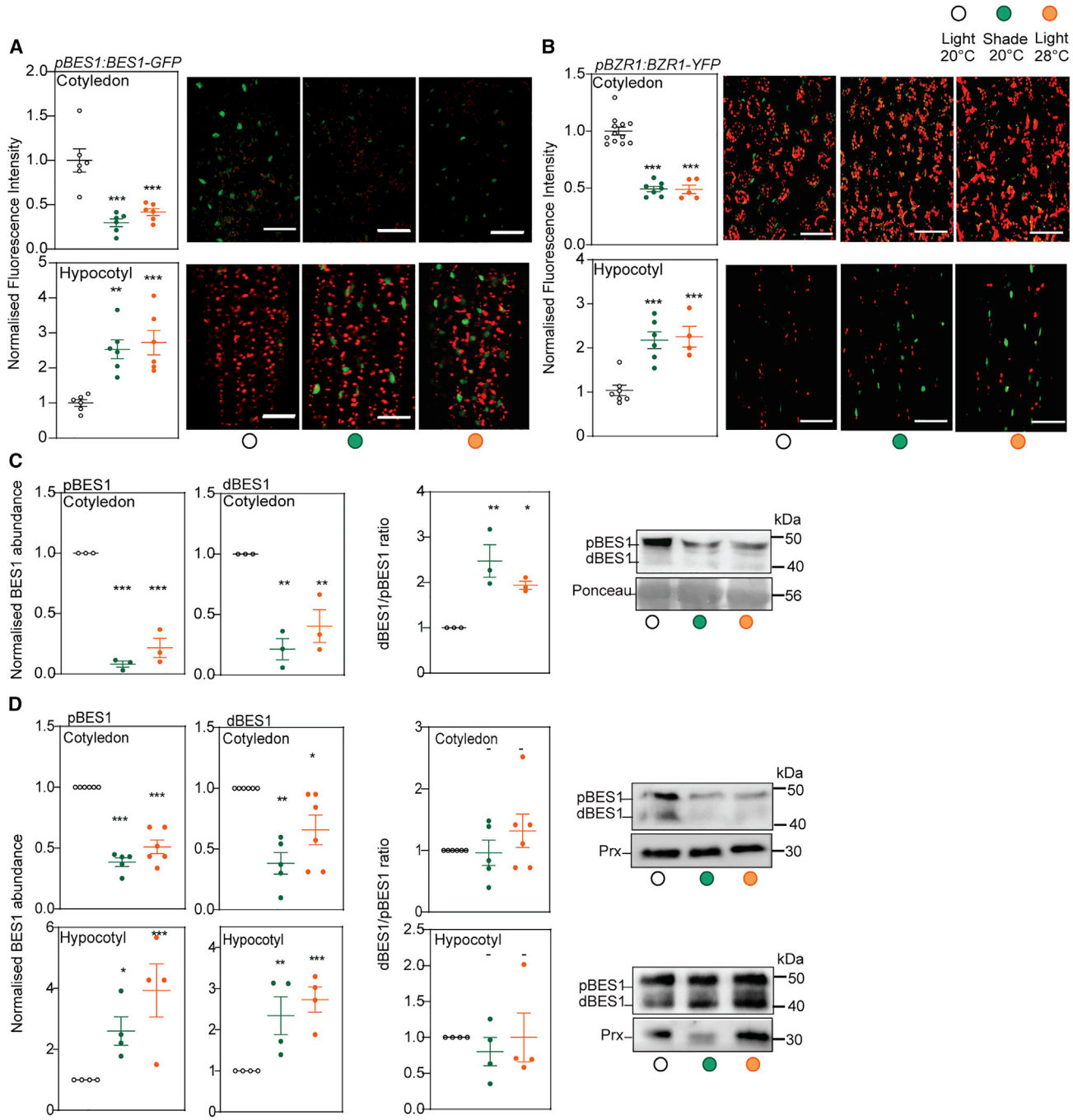


**Figure 2. BES1 and BZR1 levels decrease in the cotyledons and increase in the hypocotyl under shade or warmth**

(A and B) Nuclear fluorescence driven by *pBES1:BES1-GFP* (A) and *pBZR1:BZR1-GFP* (B) in the cotyledons and hypocotyls of *A. thaliana* seedlings in response to 4 h shade or warmth treatments.

(C and D) Abundance of phosphorylated BES1 (pBES1) and de-phosphorylated BES1 (dBES1) and dBES1/pBES1 ratio in the cotyledons of *A. thaliana* (C) and cotyledons and hypocotyls of *B. rappa* (D) after 9 h shade or warmth treatments. Prx: 2-Cys Peroxirredoxin. Data are means ± SE and individual values of 3–12 replicate boxes of seedlings and representative confocal images (scale bars, 35 μm) and protein blots. The asterisks indicate the statistical significance of the differences with the control (light at 20°C): *p < 0.05; **p < 0.01; ***p < 0.001.

Also see Figures S1 and S2.

opposite responses of BES1 in the two organs required COP1. In the hypocotyl of *pif4* mutant, BES1 showed elevated levels under control conditions and no further increment in response to shade or warmth (Figure 4F). Compared with the WT, in the *pif4* mutant, the cotyledon levels of BES1 were similar under control conditions and elevated under shade or warmth.

Please cite this article in press as: Costigliolo Rojas et al., Organ-specific COP1 control of BES1 stability adjusts plant growth patterns under shade or warmth, Developmental Cell (2022), https://doi.org/10.1016/j.devcel.2022.07.003



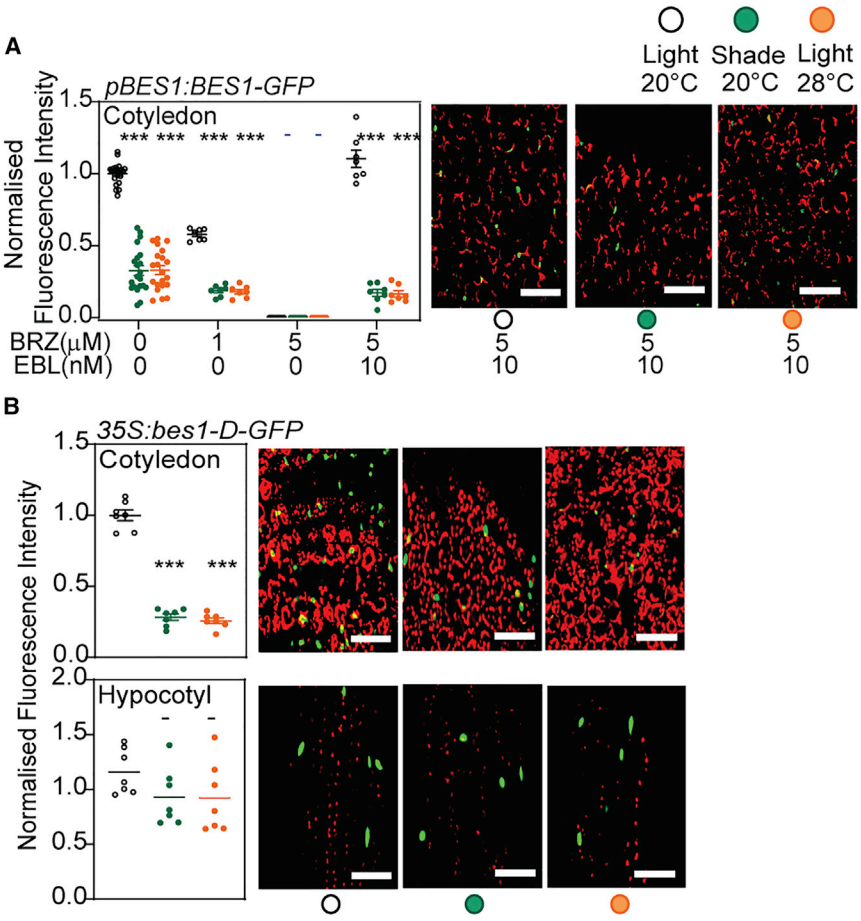


**Figure 3. Shade or warmth reduce the nuclear levels of BES1 even under conditions of impaired brassinosteroid synthesis or sensitivity**

(A) Blocking brassinosteroid synthesis with brassinazole (BRZ) does not eliminate the response of nuclear fluorescence driven by *pBES1:BES1-GFP* in the cotyledons in the presence of exogenous epibrassinolide (EBL).

(B) Nuclear fluorescence driven by *p35S:bes1-D-GFP*, which is poorly affected by brassinosteroids (Yin et al., 2002), responds to 4 h shade or warmth in the cotyledons but not in the hypocotyls of *A. thaliana* seedlings. Data are means ± SE and individual values of 6–21 replicate boxes of seedlings and representative confocal images (scale bars, 35 μm). The asterisks indicate the statistical significance of the differences between the treatments and the control (light at 20°C): *$p < 0.05$; **$p < 0.01$; ***$p < 0.001$.

Also see Figure S3.

## Shade, warmth, and PIF4 reduce *BES1* expression

To investigate whether transcriptional responses are involved in the observed changes in BES1 abundance, we analyzed *BES1* mRNA levels by real-time PCR. Shade or warmth reduced the expression of *BES1* both in the cotyledons (Figure 5A) and hypocotyl (Figure 5B). In the cotyledons, the *phyB* mutant showed reduced *BES1* expression under control conditions, i.e., showed a constitutive response to shade or warmth (Figure 5A). The *cop1* mutant showed reduced *BES1* expression under control conditions and WT expression under shade or warmth (Figure 5A). The *pif4* mutant showed elevated expression, indicating that PIF4 represses *BES1* expression (Figure 5A). The residual *BES1* expression response to shade or warmth of the *pif4* mutant could be due to the action of other PIFs. Consistently with this possibility, shade or warmth did not decrease *BES1* expression in the *pif4 pif5 pif7* triple mutant cotyledons or hypocotyl (Figure S4). This triple mutant showed reduced *BES1* expression under control conditions, which together with the *pif4* phenotype suggests positive and negative regulatory pathways linking PIFs to *BES1* (see below).

Previous analysis at the genomic level had identified *BES1* as one of the binding targets of PIF4 (Oh et al., 2014). We confirmed binding of PIF4 to different regions of the *BES1* promoter by using a PIF4 overexpressing line (Figure 5C), although weaker than observed for other targets (Figure S5). Binding was not significantly affected by the exposure of the seedlings to supplementary far-red light to lower phyB activity. We also observed binding of PIF4 to the *BES1* promoter in a quantitative one hybrid-type system in mammalian cells (Figure 5D).

We used a *trans*-activation system in *A. thaliana* protoplasts to evaluate the consequence of direct binding of PIF4 to the *BES1* promoter. The results indicate that the direct action of PIF4 is to promote *BES1* promoter activity (Figure 5E). Therefore, the negative regulation of *BES1* expression by PIF4 (revealed by the *pif4* mutant) is indirect and involves additional regulators with weaker impact in the protoplast system.

## Transcriptional effects account for PIF4 but not COP1 regulation of BES1 nuclear abundance

The increasing abundance of nuclear BES1 across *pBES1:BES1-GFP* heterozygous, homozygous, and *p35S:BES1-GFP* transgenic lines (Figure S4B) suggests that *BES1* mRNA levels are limiting for protein levels. We therefore investigated whether the reduction of *BES1* expression accounted for the effects of shade and warmth on nuclear BES1 abundance in cotyledon cells or post-transcriptional effects mediated by COP1, PIF4, and/or phyB were also involved. We used the step-wise model of multiple linear regression because from a list of plausible explanatory variables, this approach retains only those that significantly account for the response variable, pruning variables that provide redundant information. We used BES1 nuclear abundance as response variable (data from Figure 2A plus DMSO controls in Figure 6). We tested *BES1* mRNA levels (data from Figure 5A), the calculated activity of phyB (Legris et al., 2016), the nuclear levels of COP1 (Figure 4B), and the nuclear levels of PIF4 (Figure 4C) as explanatory variables. The analysis yielded significant positive effects of *BES1* mRNA levels (normalized regression coefficient: 0.26; standard error [SE]: 0.03; $p < 0.001$), indicating that the nuclear levels of

Please cite this article in press as: Costigliolo Rojas et al., Organ-specific COP1 control of BES1 stability adjusts plant growth patterns under shade or warmth, Developmental Cell (2022), https://doi.org/10.1016/j.devcel.2022.07.003



CellPress

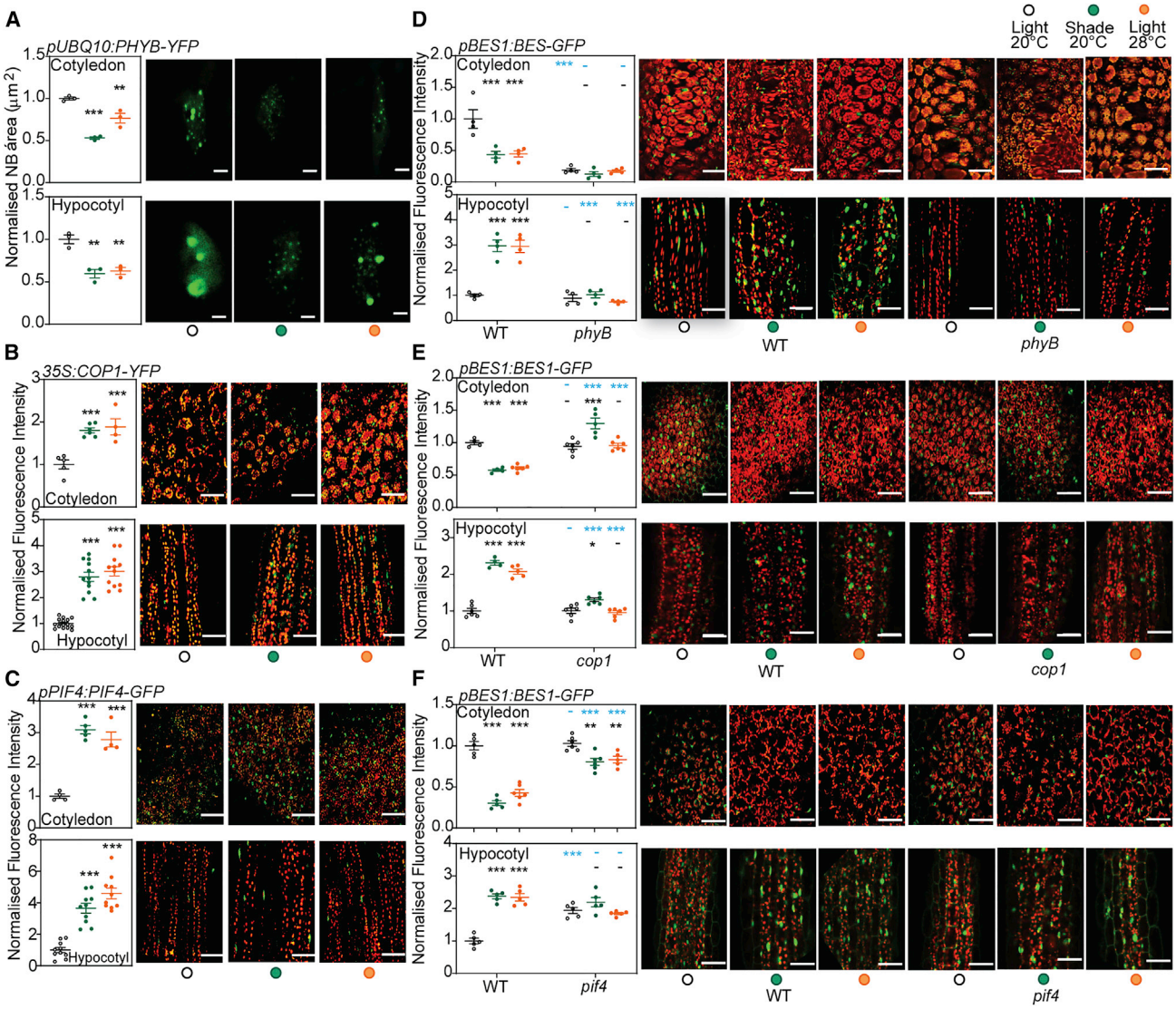


**Figure 4. Wild-type responses of BES1 nuclear levels to shade or warmth require phyB, COP1, and PIF4**

(A–C) Shade and warmth decrease phyB activity (A, phyB nuclear body [NB], area is used as a proxy of activity) and increase COP1 (B) and PIF4 (C) nuclear abundance both in the cotyledons and in the hypocotyl.

(D–F) BES1 nuclear levels in the cotyledons and in the hypocotyl of *phyB* (D), *cop1* (E), and *pif4* (F) mutant seedlings. Data are means ± SE and individual values of 3–15 replicate boxes of seedlings and representative confocal images (in A, scale bars, 3.5 μm; in B–F, scale bars, 35 μm). The asterisks indicate the statistical significance of the differences between the treatments and the control (light at 20°C) for the same genotype (black) and between the mutant and the wild type under the same condition (blue): *p < 0.05; **p < 0.01; ***p < 0.001, -, not significant.

BES1 correlate with *BES1* expression, affected by the different combinations of genotype and treatment conditions. The model also yielded significant negative effects of COP1 (normalized regression coefficient: −0.23; SE: 0.03; p < 0.001). The co-existence of *BES1* mRNA levels and COP1 nuclear levels as significant explanatory variables suggests post-transcriptional effects of COP1 on BES1 nuclear abundance. The analysis excluded PIF4 and phyB from the list of parsimonious explanatory variables due to redundancy. Both PIF4 and phyB do affect BES1 nuclear abundance (Figures 4D and 4F), but the result of the analysis indicate that these effects occurred largely via changes in *BES1* mRNA (Figure 5A), already included in the model. Having established no significant effects of PIF4 on BES1 nuclear levels downstream its control of *BES1* mRNA, we recalculated the multiple regression excluding *BES1* mRNA as explanatory variable to investigate whether the specific effect of PIF4 was important. We then obtained a significant negative effect of PIF4 (standardized regression coefficient: −0.18; SE: 0.03; p < 0.0001) and the same quantitative effect of COP1 as before (standardized regression coefficient: −0.23; SE: 0.03; p < 0.0001). Therefore, PIF4 effects on *BES1* expression and COP1-mediated post-transcriptional effects of comparable magnitude control the nuclear levels of BES1.

Please cite this article in press as: Costigliolo Rojas et al., Organ-specific COP1 control of BES1 stability adjusts plant growth patterns under shade or warmth, Developmental Cell (2022), https://doi.org/10.1016/j.devcel.2022.07.003



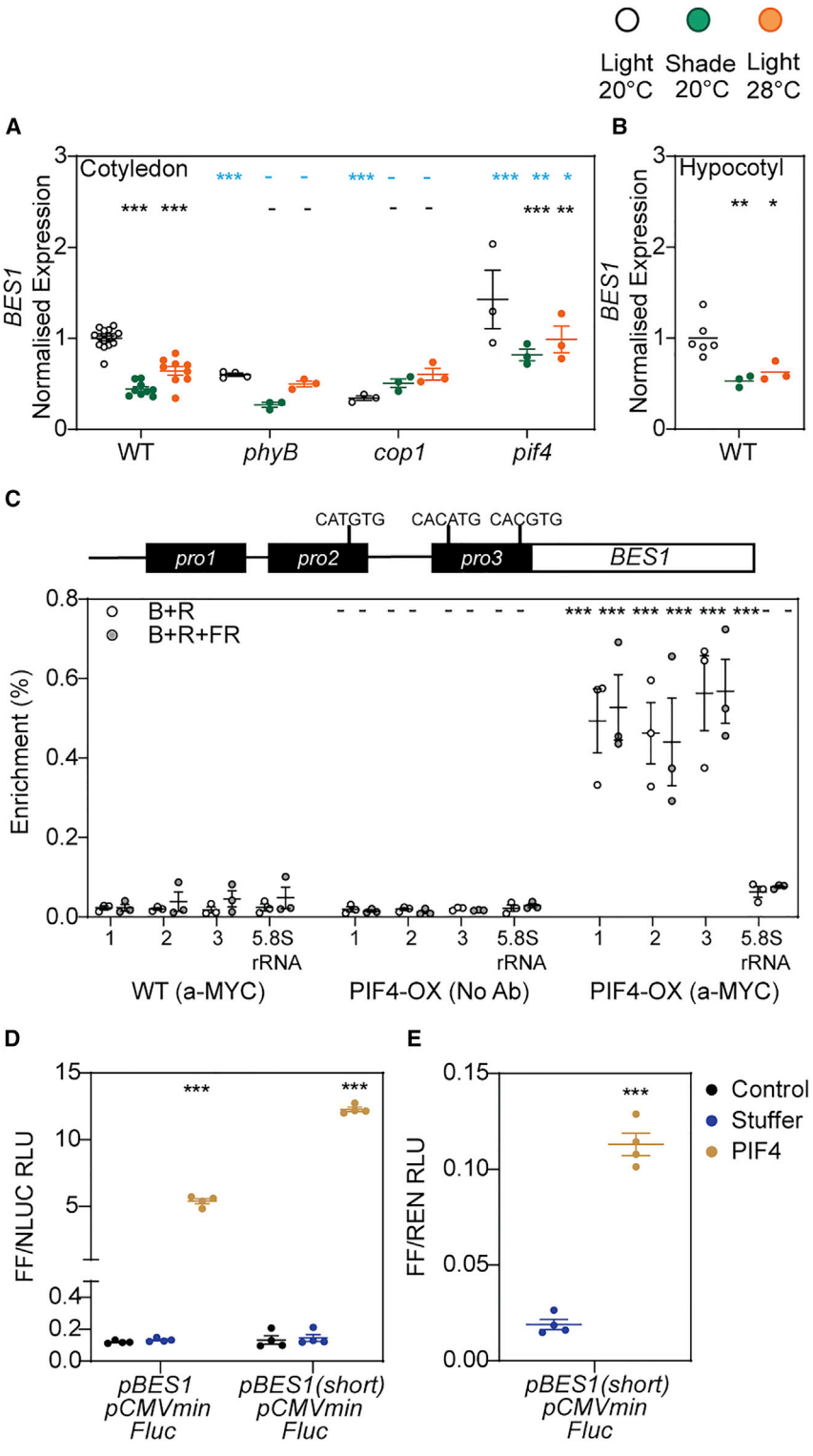


**Figure 5. Shade, warmth, and PIF4 reduce *BES1* expression**

(A) *BES1* expression in the cotyledons of wild-type, *phyB*, *cop1*, and *pif4* seedlings 4 h after transfer to shade or warmth.

(B) *BES1* expression in the hypocotyl 4 h after transfer to shade or warmth.

(C) PIF4 binds the *BES1* promoter in chromatin immunoprecipitation experiments (the seedlings were exposed to blue plus red light [B+R] without or with far-red light [B+R] to modify the activity of phyB). No Ab, no antibody.

(D) PIF4 binds the *BES1* promoter in a quantitative one hybrid-type system in mammalian cells. FF, firefly; NLUC, nanoluciferase; RLU, relative luminescent unit.

(E) *Trans*-activation system in *A. thaliana* protoplasts shows direct positive regulation of the *BES1* promoter by PIF4. REN, renilla. Data are means ± SE and individual values of 3–16 biological replicates. The asterisks indicate the statistical significance of the differences between the treatments and the control (light at 20°C) for the same genotype (A and B, black), between the mutant and the wild type under the same condition (A, blue), between the WT and PIF4-OX (C), or between the presence of staffer or PIF4 (D and E) *p < 0.05; **p < 0.01; ***p < 0.001, -, not significant.

Also see Figures S4 and S5.

## Post-translational effects of COP1 on BES1 nuclear abundance require the 26S proteasome

The effects of shade and warmth on nuclear fluorescence driven by *p35S:BES1-GFP* (Figures 6A and S6) or *p35S:bes1-D-GFP* (Figure 2F) are consistent with the occurrence of post-transcriptional effects suggested by the regression analysis. Furthermore, despite reducing BES1 levels, the application of the inhibitor of protein translation cycloheximide (CHX) did not eliminate the effects of shade, warmth, or *cop1* mutation on BES1 levels (Figure 6B), indicating the occurrence of a post-translational control of BES1 by COP1. We therefore explored the mechanisms of this control in subsequent experiments.

Since COP1 targets proteins for degradation in the 26S proteasome, COP1 could induce BES1 degradation. One of the predictions of this hypothesis is that the 26S proteasome inhibitor MG132 should increase nuclear BES1 abundance in a COP1-dependent manner in cotyledon cells. In accordance with the hypothesis, MG132 fully abrogated the decrease in nuclear BES1 abundance caused by shade or warmth, and its effects were not additive with *cop1*, i.e., MG132 did not increase BES1 in the *cop1* mutant (Figure 6C). As a control and taking into account that BES1 is also selectively targeted to degradation in the autophagy pathway (Nolan et al., 2017), we applied the inhibitor of cysteine peptidases E64. The application of E64 also elevated BES1 abundance, but contrary to MG132, the effects of *cop1* and E64 were additive (Figure S7). Consistently with the notion that the effects of

Please cite this article in press as: Costigliolo Rojas et al., Organ-specific COP1 control of BES1 stability adjusts plant growth patterns under shade or warmth, Developmental Cell (2022), https://doi.org/10.1016/j.devcel.2022.07.003



CellPress

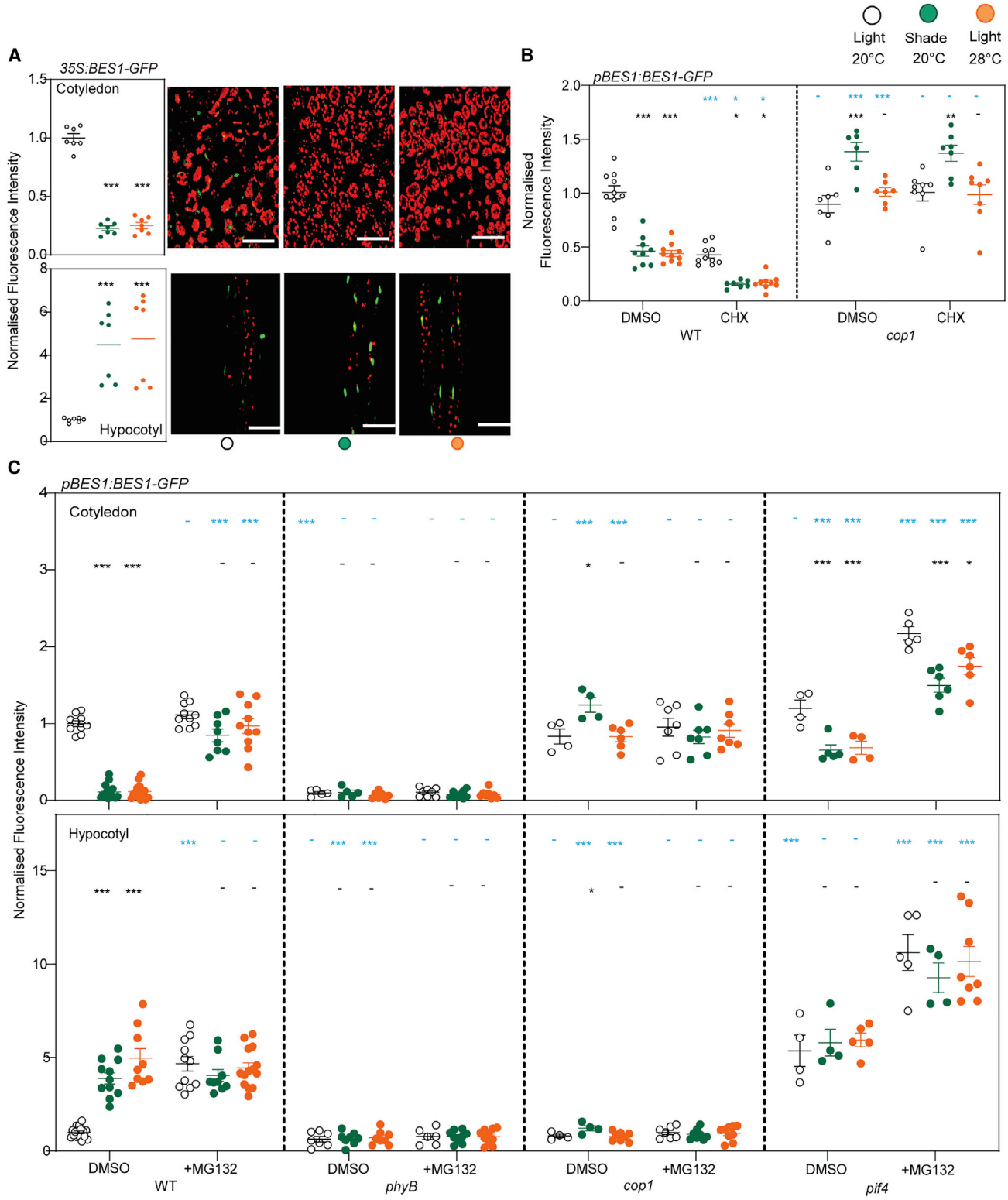


**Figure 6. Post-translational effects of COP1 on BES1 nuclear abundance require 26S proteasome activity**

(A) The responses of nuclear fluorescence driven by *p35S:BES1-GFP* in the cotyledons and hypocotyls of *A. thaliana* seedlings to 4 h shade or warmth treatments demonstrate the occurrence of a post-transcriptional control.

(B) The inhibitor of protein translation cycloheximide (CHX) does not eliminate nuclear BES1 responses to shade and warmth and has no effect in *cop1*.

*(legend continued on next page)*

PIF4 on nuclear BES1 abundance are largely accounted for by changes in *BES1* expression, the positive effects of the *pif4* mutation and MG132 treatment were additive (Figure 6C). Since the *phyB* mutation lowers *BES1* expression, MG132 did not rescue the low BES1 nuclear levels of this mutant (Figure 6C).

In contrast to the negative effects in cotyledon cells, in the hypocotyl, COP1 was required for the enhanced BES1 abundance caused by shade and warmth (Figures 3E and 6C) and MG132 caused a constitutive response to shade or warmth by elevating BES1 levels under control conditions (Figure 6C), indicating that the signaling circuits involving COP1 are different in cotyledons and hypocotyls. Conversely, the patterns of the *pif4* and *phyB* mutants were similar in the cotyledons and hypocotyl (Figure 6C).

## COP1 physically interacts with BES1

Since shade or warmth reduce the nuclear abundance of BES1 in a proteasome and COP1-dependent manner, we investigated if COP1 physically interacts with BES1. We engineered a split transcription factor, quantitative two-hybrid-type system in mammalian cells (Müller et al., 2014). This orthogonal, heterologous system allows to assess the interaction of plant proteins in a targeted way, in the absence of other plant proteins that might interfere, and to identify the minimal components needed for such interaction. In addition, it is possible to perform the experiments in the presence or absence of light and to add subsequent proteins to evaluate the formation of complexes. We observed interaction between COP1 and BES1 (Figure 7A). This interaction did not require SPA1. COP1 interacted with BES1 in the presence of SPA1 (Figure 7A) required for COP1 *in vivo* E3 ligase activity (Ponnu and Hoecker, 2021), but the presence of SPA1 reduced the signal (SPA1 interacts very strongly with COP1 competing with the formation of COP1-BES1). phyB (in its active or inactive form) did not interfere.

In *A. thaliana* cells, BES1-GFP driven by its endogenous promoter localized diffusely to the nucleoplasm (Figure 7B). The confocal images of hemizygous seedlings bearing the *pBES1:BES1-GFP* and *p-COP1-mCHERRY-COP1* transgenes demonstrate co-occurrence (spatial overlap) of BES1 and COP1 in the nuclei of cotyledon cells (Figure 7C). Resembling the observations in *A. thaliana*, YFP-BES1 localized diffusely to the nucleoplasm of *N. benthamiana* cells, and expression of DsRED-COP1-HA did not significantly affect this pattern (Figure 7D). However, DsRED-COP1-HA formed large and numerous nuclear bodies when co-expressed with c-myc-SPA1. These nuclear bodies dragged YFP-BES1 into them (ratio between YFP-BES1 fluorescence ratio inside and outside the DsRED-COP1-HA nuclear bodies larger than 1, Figure 7D), indicating the occurrence of co-localization in this system, where SPA1 concentrates COP1 and COP1 concentrates BES1.

To investigate the interaction of BES1 and COP1 in planta, we used co-immunoprecipitation assays in leaves of *N. benthamiana* co-expressing DsRED-COP1-HA and YFP-BES1 (with or without c-myc-SPA1). Anti-GFP antibodies pulled down DsRED-COP1-HA from leaf extracts that co-expressed both proteins, but not from extracts of control leaves expressing DsRED-COP1-HA alone (Figure 7E). Bimolecular fluorescence complementation of YFC-BES1 and YFN-COP1 in leaves of *N. benthamiana* confirmed the interaction between COP1 and BES1 (Figure 7F). Both approaches showed that the interaction occurs with or without co-expression of c-myc-SPA1 (Figures 7E and 7F).

## BES1 promotes hypocotyl and cotyledon growth

The loss-of-function *bes1-1* mutant showed reduced growth of the cotyledons and hypocotyl, which did not respond to shade or warmth (Figures 8A, 8B, and S8A). An independent allele confirmed the cotyledon phenotype (Figures 8C, S8A, and S8B). The *phyB* mutant showed reduced cotyledon expansion but enhanced hypocotyl growth, retaining partial responses to shade and warmth (Figure 8B). The *cop1* and *pif4* mutations did not affect cotyledon expansion under control conditions and enhanced cotyledon expansion under shade and warmth (Figure 8B). As expected, these mutants showed reduced hypocotyl growth rates, which were less responsive to shade and warmth. We observed a significant correlation between BES1 levels and cotyledon expansion (standardized regression coefficient: 0.23; SE: 0.02; $p < 0.0001$). This correlation accounts for a significant proportion of the observed cotyledon growth mutant phenotypes. Figure 8D summarizes the mechanisms of control of cotyledon expansion reported here. If the model is correct, MG132 should enhance cotyledon expansion in the WT but not in the *cop1* mutant. In addition, enhanced *BES1* expression in the *p35S:BES1-GFP* transgenic should increase cotyledon expansion, and this line should respond to shade and warmth. The results were consistent with both expectations (Figures 8E and 8F).

The loss-of-function *bzr1* mutant also reduced cotyledon expansion and its response to shade and warmth (Figures S8C and S8D). The effects of the *bes1* and *bzr1* mutations were not additive, which is consistent with the reduced levels of BZR1 in *bes1* mutants (Jeong et al., 2015; Figure S8E). Although under control conditions, the final size of the cotyledons is larger in gain-of-function *bes1-1D* and *bzr1-1D* mutants than in the WT (Figure S8F), and the rate of expansion on day 4 was reduced (Figure S8G). In *bes1-1D* and *bzr1-1D* mutants and *DWF4* overexpressors, shade and warmth promoted rather than inhibited cotyledon expansion (Figure S8G), indicating that WT cotyledon expansion patterns require tight regulation of BES1 and BZR1 activities. Finally, since cryptochrome 1 (cry1) reduces COP1 (Lau and Deng, 2012) and PIF4 (Boccaccini et al., 2020; Ma et al., 2016; Pedmale et al., 2016) activities, if our model (Figure 8D) is correct, the *cry1* mutation should reduce cotyledon expansion under control conditions. The results confirmed this expectation (Figure S8H).

## DISCUSSION

We report that organ-specific changes in BES1 and BZR1 nuclear levels mediate cotyledon-growth responses to shade and

(C) Effects of MG132 and its interaction with *phyB*, *cop1*, and *pif4* mutations. Data are means ± SE and individual values of 4–16 replicate boxes of seedlings. The asterisks indicate the statistical significance of the differences between the treatments and the control (light at 20° C) for the same genotype (black) and between the mutant and the wild type under the same condition (blue): *$p < 0.05$; **$p < 0.01$; ***$p < 0.001$, -, not significant.
Also see Figures S6 and S7.

Please cite this article in press as: Costigliolo Rojas et al., Organ-specific COP1 control of BES1 stability adjusts plant growth patterns under shade or warmth, Developmental Cell (2022), https://doi.org/10.1016/j.devcel.2022.07.003



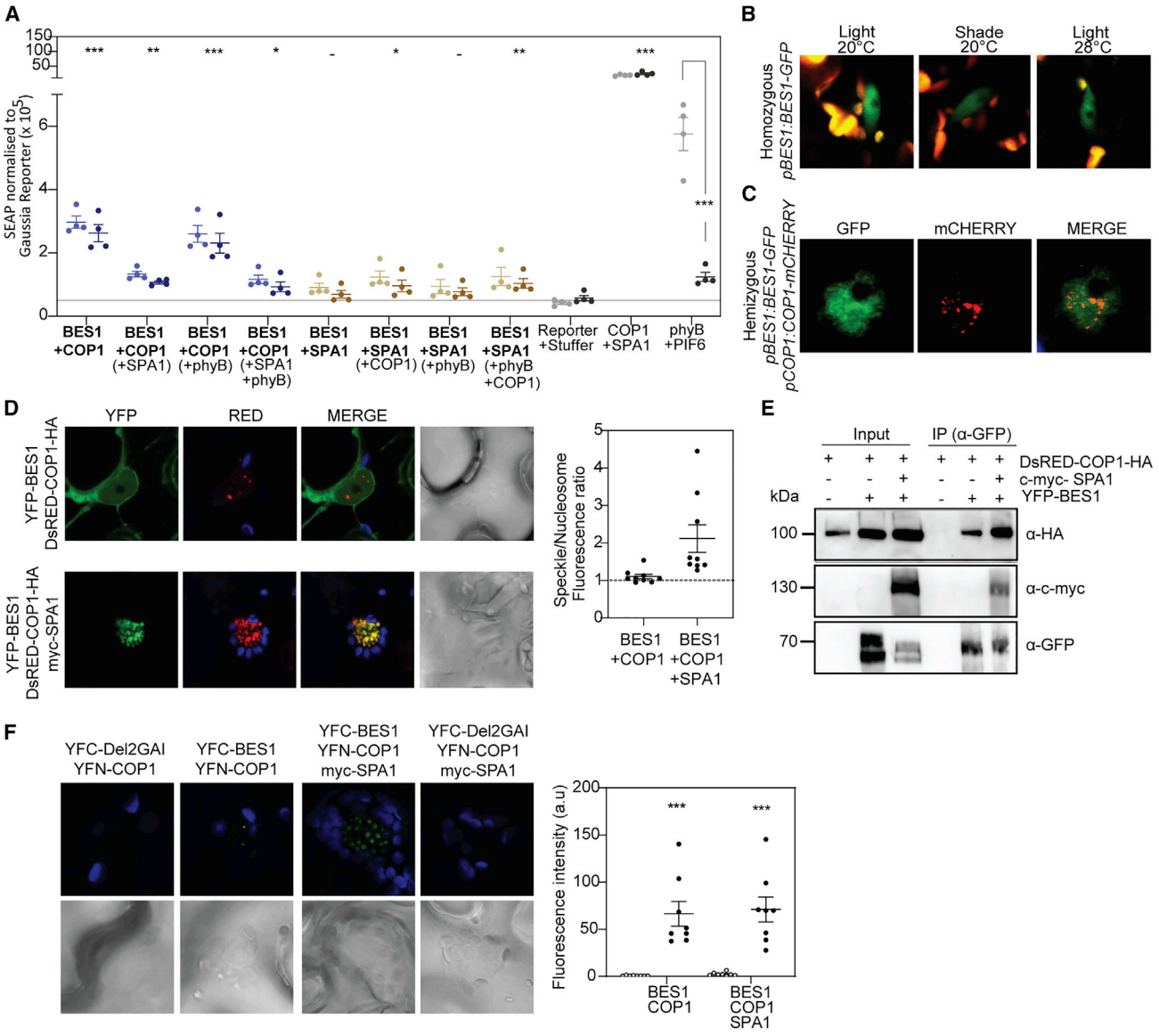


**Figure 7. BES1 physically interacts with COP1**

(A) Analysis of the interaction of BES1 with COP1 and SPA1 in a split-transcription factor, mammalian-hybrid-like assay in HEK293T cells. SEAP, secreted alkaline phosphatase. Clear and dark colored boxes correspond to samples exposed to red light or darkness, respectively.

(B) BES1 diffusely localizes to the nucleosome of *A. thaliana* cells, and this is not affected by shade or warmth.

(C) Co-occurrence of BES1 and COP1 in homozygous (F1) seedlings bearing the *pBES1:BES1-GFP* and the *pCOP1:mCHERRY-COP1* transgenes in *A. thaliana*.

(D) Co-localization of YFP-BES1 with DsRED-COP1-HA and c-myc-SPA1 in leaves of *N. benthamiana*.

(E) Coimmunoprecipitation assays showing interactions in planta. YFP-BES1 was transiently expressed in leaves of *N. benthamiana* together with DsRED-COP1-HA (with or without the COP1 complex partner c-myc-SPA1). Proteins were immunoprecipitated with anti-GFP antibody-coated paramagnetic beads.

(F) Fluorescence per unit nuclear body area (a.u., arbitrary units) in bimolecular fluorescence complementation experiments with YFC-BES1 and YFN-COP1 in the presence or the absence of myc-SPA1 in leaves of *N. benthamiana*. For each condition, we show fluorescence intensity within a fixed area out (close to zero) and inside the speckles. In (D) and (F), blue fluorescence corresponds to the chloroplasts. Data are means ± SE and individual values of 3–8 biological replicates and representative images. Samples exposed to red light or darkness were pooled for this analysis (not significantly different, except for phyB+PIF6). The asterisks indicate the significance of the differences with the reporter plus staffer control: *p < 0.05; **p < 0.01; ***p < 0.001, -, not significant.

warmth. These environmental cues caused a rapid reduction in the rate of cotyledon expansion, which paralleled the increase in the rate of hypocotyl extension both in *A. thaliana* and *B. napus* (Figures 1B–1D and S1B). In cotyledon cells, shade and warmth decreased the nuclear levels of BES1 and BZR1 (Figures 1A and 2). The *bes1* and *bzr1* mutants showed reduced cotyledon expansion and reduced (*bzr1*) or null (*bes1*) responses to shade or warmth (Figures 8A–8C and S8), and gain-of-function *bes1-D* and *bzr1-D* mutants showed distorted cotyledon growth patterns (Figure S8). Gibberellins (Josse et al., 2011) and auxin signaling (Enders et al., 2017; Lewis et al., 2009; Strader et al., 2010) were essential for WT cotyledon expansion responses

Please cite this article in press as: Costigliolo Rojas et al., Organ-specific COP1 control of BES1 stability adjusts plant growth patterns under shade or warmth, Developmental Cell (2022), https://doi.org/10.1016/j.devcel.2022.07.003



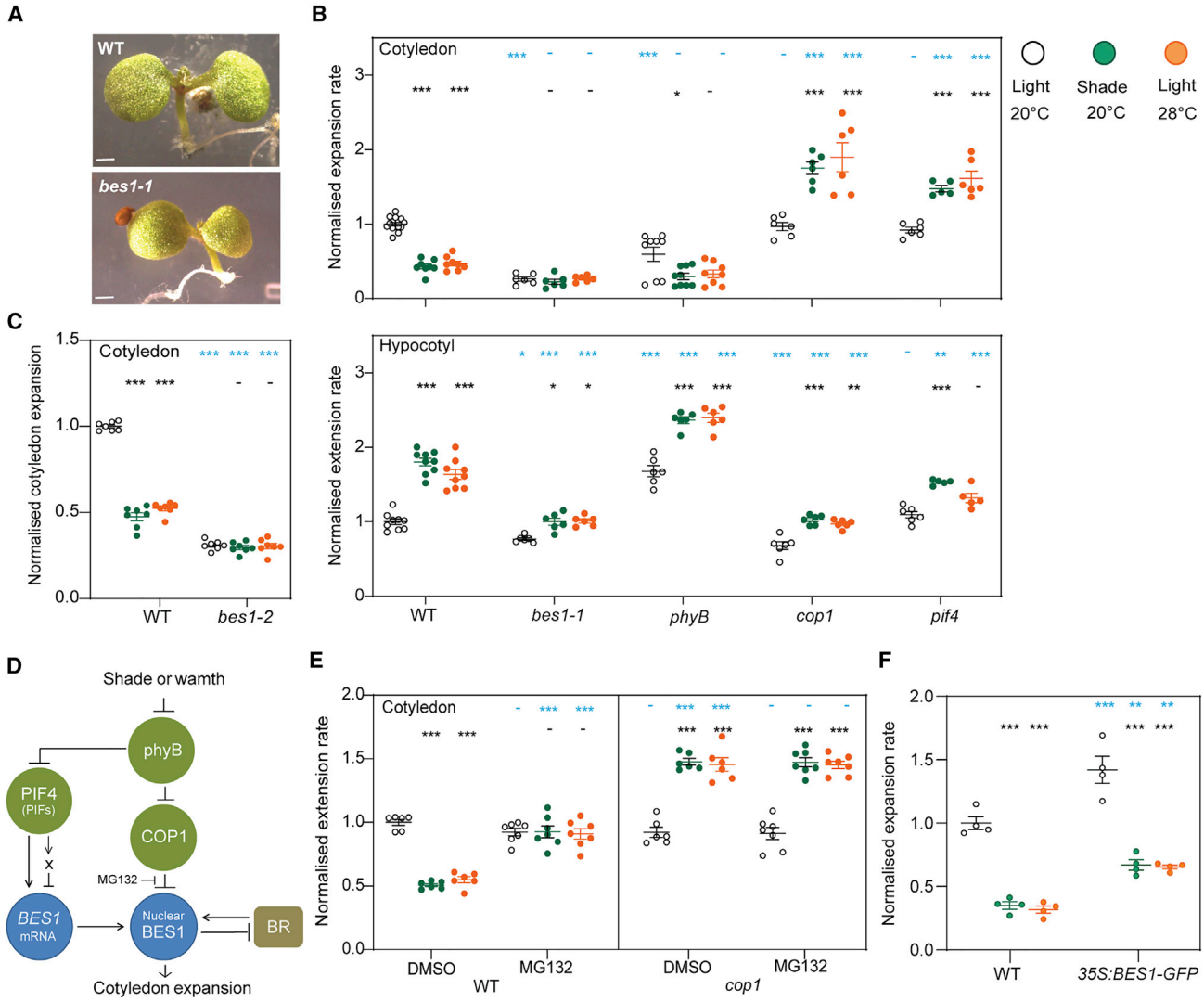


**Figure 8. BES1 promotes hypocotyl and cotyledon growth**

(A) Reduced cotyledon size in 7-day-old seedlings of the *bes1* mutant (scale bars, 1 mm).

(B) Cotyledon expansion and hypocotyl extension rates in the wild type and the *bes1*, *phyB*, *cop1*, and *pif4* mutants during the 9 h exposure to shade or warmth.

(C) Cotyledon expansion in an independent allele of *bes1*.

(D) Model of the mechanisms of control of cotyledon expansion by shade and warmth reported here.

(E and F) Test of the model: MG132 (E) and enhanced *BES1* expression (F) increase cotyledon expansion. Data are means ± SE and individual values of 5–14 replicate boxes of seedlings. The asterisks indicate the statistical significance of the differences between the treatments and the control (light at 20°C) for the same genotype (black) and between the mutant and the wild type under the same condition (blue): *p < 0.05; **p < 0.01; ***p < 0.001, -, not significant.

Also see Figure S8.

(Figures 1 and S1). However, the status of the gibberellin-DELLA pathway did not respond to shade or warmth in epidermal cells of the cotyledons (Figure 1A). Furthermore, exogenous auxin did not inhibit cotyledon growth, despite elevating auxin signaling status in epidermal cell to the level reached under shade or warmth (Figure 1B).

Growth (Figures 1D and S1) and BES1 abundance (Figure 3A) responses to shade or warmth required brassinosteroids. The levels of active hormone did not decrease in whole cotyledons (Figure S3). In addition, shade and warmth reduced the nuclear abundance of the BES1-D protein (Figure 3B), which is poorly sensitive to brassinosteroids (Yin et al., 2002). They also reduced the nuclear abundance of BES1 in the presence of a saturating dose of brassinosteroid synthesis inhibitor (Figure 3A). Although these results do not rule out the involvement of transient or localized changes in brassinosteroids in the control of BES1, they demonstrate the occurrence of additional mechanisms of regulation. In fact, shade and warmth reduced phyB activity in the cotyledons (Figure 4A, smaller phyB nuclear bodies is a manifestation of this change) setting into motion two convergent pathways of action on BES1 levels, respectively, involving PIF4 and COP1.

phyB induces PIF4 degradation (Park et al., 2018; Pham et al., 2018a); therefore, in the first pathway, shade and warmth

Please cite this article in press as: Costigliolo Rojas et al., Organ-specific COP1 control of BES1 stability adjusts plant growth patterns under shade or warmth, Developmental Cell (2022), https://doi.org/10.1016/j.devcel.2022.07.003





increased of PIF4 nuclear abundance in cotyledon cells (Figure 4C), and PIF4 repressed *BES1* expression. In support of this pathway, the *pif4* mutant showed enhanced nuclear levels in the cotyledons (Figure 3F), accounted for by enhanced levels of *BES1* expression (see regression analysis in Results). PIF4 bound the *BES1* promoter in plant and mammalian cells (Figures 5C and 5D), and *trans*-activation experiments with *A. thaliana* protoplasts revealed that the direct action of PIF4 is to enhance *BES1* promoter activity (Figure 5E). Therefore, the inhibition of *BES1* expression evidenced by the enhanced expression in *pif4* compared with the WT could involve, for instance, PIF4 promotion of the expression of a repressor of *BES1* expression, enhanced binding of this repressor to the *BES1* promoter in the presence of PIF4 and/or changed PIF4 activity due to heterodimerization.

phyB reduces COP1 activity (Lau and Deng, 2012; Sheerin et al., 2015); therefore, in the second pathway, shade or warmth increased COP1 nuclear levels in cotyledon cells (Figure 4B) to directly target BES1 to degradation in the proteasome. In support of this pathway, shade or warmth reduced the nuclear levels of BES1 under the control of a constitutive promoter (Figure 6A), indicating the occurrence of post-transcriptional regulation. Furthermore, the *cop1* mutant showed enhanced BES1 nuclear levels in cotyledon cells under shade or warmth (Figure 4E) without affecting *BES1* expression under these conditions (Figure 4A). A statistical model pointed to post-transcriptional regulation by COP1, and consistently with this interpretation, the use of CHX to block translation did not eliminate the effects of shade or warmth or of the *cop1* mutation on BES1 nuclear levels (Figure 6B). As observed for the *cop1* mutation, the proteasome 26S inhibitor MG132 increased the abundance of BES1, and these effects where redundant (Figure 6C). On the contrary, the inhibitor of cysteine proteases E64, which also increased nuclear BES1, had additive effects with the *cop1* mutation (Figure S9). Finally, COP1 physically interacted with BES1 in mammalian cells and *in planta* (Figure 7).

COP1 also interacts physically with BZR1 favoring its proteasome-dependent degradation (Kim et al., 2014). In *A. thaliana*, the decay of BES1 in the cotyledons exposed to shade or warmth (Figure 2C) and the reduction of BZR1 in whole dark-grown seedlings (Kim et al., 2014) is somewhat stronger for the phosphorylated than the de-phosphorylated form. The increased proportion of the de-phosphorylated form (despite its decreased abundance) had been proposed to enhance BZR1 activity to promote hypocotyl growth (Kim et al., 2014). However, the current observations that BZR1 decreases in the cotyledon and not in the hypocotyl (Figure 2) and that decreased BZR1 activity plays a role in the reduction of cotyledon expansion (Figure S9) offer a reinterpretation. According to this alternative view, as shown here for BES1, COP1 would decrease BZR1 abundance in the cotyledons to reduce the expansion of this organ under shade, warmth, or in darkness.

Hypocotyl growth responses to shade or warmth depend on brassinosteroid signaling (Ibañez et al., 2018; Kozuka et al., 2010; Luccioni et al., 2002; Oh et al., 2012; Stavang et al., 2009), and the *bes1* loss-of-function mutant showed impaired hypocotyl growth responses to these cues (Figure 8B). Shade or warmth increased the nuclear levels of BES1 in hypocotyl cells (Figures 2A, 4D–4F, and 5D), although reducing *BES1* expression (Figure 5B), indicating the occurrence of a post-transcriptional control. Consistently, these cues also enhanced nuclear fluorescence driven by *p35S:BES1-GFP* in the hypocotyl (Figure 6A) as reported for *p35S:BZR1-GFP* in response to temperature (Ibañez et al., 2018). Noteworthy, in contrast to the cotyledons, the *cop1* mutation and MG132 redundantly reduced BES1 in hypocotyl cells (Figures 4E and 6C). Thus, we propose that COP1 reduces the activity of a negative regulator of BES1 stability in the hypocotyl. This regulator remains to be elucidated, but potential candidates include the kinase BIN2 (Ling et al., 2017) and the E3 ligase SINAT (Yang et al., 2017). The lack of shade or warmth effects on the fluorescence driven by *p35S:bes1-D-GFP* in the hypocotyl (Figure 3B) would be consistent with a role of BIN2. Clearly, the relationship between COP1 and its targets is strongly context dependent. In addition to the organ-dependent effects on BES1, under shade or warmth, COP1 rapidly targets to degradation RGA in the hypocotyl (Blanco-Touriñán et al., 2020), but not in the cotyledons (Figure 1A), and the COP1-SPA complex stabilizes PIF5 in darkness but favors its degradation in the light (Pham et al., 2018b). In addition to COP1, the canonical control of BES1 could operate during warm nights, when increased expression of brassinosteroid synthesis genes takes place (Purlyte et al., 2018).

Photosynthetic light interception and transpiration of plant canopies depend on leaf area and impact on the biodiversity of natural ecosystems and the productivity of food crops. Therefore, in the current climate emergency, it is crucial to understand how the light and temperature environment affects leaf expansion. Neighbor cues reduce the expansion of the blade in post-embryonic leaves of *A. thaliana* by limiting cell division during the proliferative phase and limiting cell expansion at later stages (Romanowski et al., 2021). The reduced cell proliferation involves an auxin-cytokinin pathway (Carabelli et al., 2007). Our work reveals a mechanism of control of expansion of cotyledon cells shared by shade and warmth. It will be important to test this mechanism in post-embryonic leaves. This novel mechanism involves downregulation of BES1 at the transcriptional level by PIF4 and at the post-transcriptional level by COP1 (Figure 8D). The same players participate in the control of hypocotyl growth, but there COP1 enhances, rather than decrease, BES1 nuclear abundance.

## STAR★METHODS

Detailed methods are provided in the online version of this paper and include the following:

- KEY RESOURCES TABLE
- RESOURCE AVAILABILITY
  - Lead contact
  - Materials availability
  - Data and code availability
- EXPERIMENTAL MODEL AND SUBJECT DETAILS
  - Plant Material
- METHOD DETAILS
  - Growth conditions and treatments
  - Hypocotyl and cotyledon growth rate
  - Confocal microscopy
  - Pharmacological treatments

- Protein blots
- Quantitative reverse transcriptase-PCR
- Brassinosteroid analysis
- Chromatin immunoprecipitation (ChIP)
- One-hybrid in mammalian cells
- Protoplast transactivation
- Co-immunoprecipitation
- Bi-molecular fluorescence complementation
- Co-localization assays in *N. benthamiana*
- Protein-protein interaction assays in mammalian cells

● QUANTIFICATION AND STATISTICAL ANALYSIS

## SUPPLEMENTAL INFORMATION

Supplemental information can be found online at https://doi.org/10.1016/j.devcel.2022.07.003.

## ACKNOWLEDGMENTS

We thank Patrick Fischbach (University of Düsseldorf) for assistance with cloning. We thank Yanhai Yin (Iowa State University) for his kind provision of BES1 antibody and Masato Saito and Hiroo Fukuda (University of Tokyo) for their kind provision of *bes1* and *bzr1* loss-of-function mutant seeds, Ana Caño-Delgado (Center for Research in Agricultural Genomics, Barcelona) for her kind provision of *p35S:BES1-GFP* and *p35S:bes1-D-GFP* seeds and Andreas Hiltbrunner (University of Freiburg) for his kind provision of *pCOP1:COP1-mCHERRY* seeds. This work was supported by grants from the University of Buenos Aires (grant no. 20020170100505BA to J.J.C.), Agencia Nacional de Promoción Científica y Tecnológica (grant numbers PICT-2019-2019-01354 to J.J.C., PICT-2019-2019-2252 to C.C.R., and PICT2016-2234 to S.M.-G.), European Regional Development Fund Project "Centre for Experimental Plant Biology" (grant number CZ.02.1.01/0.0/0.0/16_019/0000738 to D.T.), National Research Foundation of Korea (grant number 2018R1A3B1052617 to G.C.), Spanish Ministry of Science and Innovation (grant number PID2019-109925GB-I00 to D.A.), Generalitat Valenciana (grant number PROMETEO/2019/021 to M.A.B.), and Deutsche Forschungsgemeinschaft (DFG, German Research Foundation) under Germany's Excellence Strategy CEPLAS—EXC-2048/1—Project no. 390686111, the iGRAD Plant (IRTG 1525) to M.D.Z., and NEXTplant (GRK 2466) to J.S. and M.D.Z.

## AUTHOR CONTRIBUTIONS

Investigation, C.C.-R., L.B., J.O., S.R.M., D.T., E.G.M., J.S., M.G.H., T.F., and D.A.; conceptualization, C.C.-R. and J.J.C.; writing, J.J.C. with input from C.C.-R., D.T., M.A.B., G.C., M.S., S.M.-G., D.A., and M.D.Z.; funding acquisition, C.C.-R., D.T., G.C., D.A., M.D.Z., and J.J.C., visualization, C.C.-R. and J.J.C.; formal analysis, C.C.-R. and J.J.C.; supervision, D.T., M.A.B., G.C., M.S., S.M.-G., D.A., M.D.Z., and J.J.C.

## DECLARATION OF INTERESTS

The authors declare no competing interests.

Received: July 1, 2021
Revised: February 16, 2022
Accepted: July 5, 2022
Published: July 27, 2022

## REFERENCES

Achard, P., Cheng, H., De Grauwe, L., Decat, J., Schoutteten, H., Moritz, T., Van Der Straeten, D., Peng, J., and Harberd, N.P. (2006). Integration of plant responses to environmentally activated phytohormonal signals. Science *311*, 91–94.

Baaske, J., Gonschorek, P., Engesser, R., Dominguez-Monedero, A., Raute, K., Fischbach, P., Müller, K., Cachat, E., Schamel, W.W.A., Minguet, S., et al. (2018). Dual-controlled optogenetic system for the rapid down-regulation of protein levels in mammalian cells. Sci. Rep. *8*, 15024.

Bai, M.Y., Shang, J.X., Oh, E., Fan, M., Bai, Y., Zentella, R., Sun, T.P., and Wang, Z.Y. (2012). Brassinosteroid, gibberellin and phytochrome impinge on a common transcription module in Arabidopsis. Nat. Cell Biol. *14*, 810–817.

Ballaré, C.L., and Pierik, R. (2017). The shade-avoidance syndrome: multiple signals and ecological consequences. Plant Cell Environ. *40*, 2530–2543.

Bellstaedt, J., Trenner, J., Lippmann, R., Poeschl, Y., Zhang, X., Friml, J., Quint, M., and Delker, C. (2019). A mobile auxin signal connects temperature sensing in cotyledons with growth responses in hypocotyls. Plant Physiol. *180*, 757–766.

Beuchat, J., Scacchi, E., Tarkowska, D., Ragni, L., Strnad, M., and Hardtke, C.S. (2010). BRX promotes Arabidopsis shoot growth. New Phytol. *188*, 23–29.

Blanco-Touriñán, N., Legris, M., Minguet, E.G., Costigliolo-Rojas, C., Nohales, M.A., Iniesto, E., García-León, M., Pacín, M., Heucken, N., Blomeier, T., et al. (2020). COP1 destabilizes DELLA proteins in Arabidopsis. Proc. Natl. Acad. Sci. USA *117*, 13792–13799.

Blomeier, T., Fischbach, P., Koch, L.A., Andres, J., Miñambres, M., Beyer, H.M., and Zurbriggen, M.D. (2021). Blue light-operated CRISPR/Cas13b-mediated mRNA knockdown (lockdown). Adv. Biol. (Weinh) *5*, e2000307.

Boccaccini, A., Legris, M., Krahmer, J., Allenbach-Petrolati, L., Goyal, A., Galvan-Ampudia, C.G., Vernoux, T., Karayekov, E., Casal, J.J., and Fankhauser, C. (2020). Low blue light enhances phototropism by releasing cryptochrome 1-mediated inhibition of PIF4 expression. Plant Physiol. *183*, 1780–1793.

Bou-Torrent, J., Galstyan, A., Gallemí, M., Cifuentes-Esquivel, N., Molina-Contreras, M.J., Salla-Martret, M., Jikumaru, Y., Yamaguchi, S., Kamiya, Y., and Martínez-García, J.F. (2014). Plant proximity perception dynamically modulates hormone levels and sensitivity in Arabidopsis. J. Exp. Bot. *65*, 2937–2947.

Carabelli, M., Possenti, M., Sessa, G., Ciolfi, A., Sassi, M., Morelli, G., and Ruberti, I. (2007). Canopy shade causes a rapid and transient arrest in leaf development through auxin-induced cytokinin oxidase activity. Genes Dev. *21*, 1863–1868.

Casal, J.J. (2013). Photoreceptor signaling networks in plant responses to shade. Annu. Rev. Plant Biol. *64*, 403–427.

Casal, J.J., and Balasubramanian, S. (2019). Thermomorphogenesis. Annu. Rev. Plant Biol. *70*, 321–346.

Choe, S., Fujioka, S., Noguchi, T., Takatsuto, S., Yoshida, S., and Feldmann, K.A. (2001). Overexpression of DWARF4 in the brassinosteroid biosynthetic pathway results in increased vegetative growth and seed yield in Arabidopsis. Plant J. *26*, 573–582.

Chory, J., Nagpal, P., and Peto, C.A. (1991). Phenotypic and genetic analysis of det2, a new mutant that affects light-regulated seedling development in Arabidopsis. Plant Cell *3*, 445–459.

Chung, B.Y.W., Balcerowicz, M., Di Antonio, M., Jaeger, K.E., Geng, F., Franaszek, K., Marriott, P., Brierley, I., Firth, A.E., and Wigge, P.A. (2020). An RNA thermoswitch regulates daytime growth in Arabidopsis. Nat. Plants *6*, 522–532.

De Lucas, M., Davière, J.M., Rodríguez-Falcón, M., Pontin, M., Iglesias-Pedraz, J.M., Lorrain, S., Fankhauser, C., Blázquez, M.A., Titarenko, E., and Prat, S. (2008). A molecular framework for light and gibberellin control of cell elongation. Nature *451*, 480–484.

de Wit, M., Ljung, K., and Fankhauser, C. (2015). Contrasting growth responses in lamina and petiole during neighbor detection depend on differential auxin responsiveness rather than different auxin levels. New Phytol. *208*, 198–209.

Deng, X.W., Caspar, T., and Quail, P.H. (1991). cop1: a regulatory locus involved in light-controlled development and gene expression in Arabidopsis. Genes Dev. *5*, 1172–1182.

Earley, K.W., Haag, J.R., Pontes, O., Opper, K., Juehne, T., Song, K., and Pikaard, C.S. (2006). Gateway-compatible vectors for plant functional genomics and proteomics. Plant J. *45*, 616–629.

Enders, T.A., Frick, E.M., and Strader, L.C. (2017). An Arabidopsis kinase cascade influences auxin-responsive cell expansion. Plant J. *92*, 68–81.

Espinosa-Ruiz, A., Martínez, C., De Lucas, M., Fàbregas, N., Bosch, N., Caño-Delgado, A.I., and Prat, S. (2017). TOPLESS mediates brassinosteroid control of shoot boundaries and root meristem development in *Arabidopsis thaliana*. Development *144*, 1619–1628.

Feng, S., Martinez, C., Gusmaroli, G., Wang, Y., Zhou, J., Wang, F., Chen, L., Yu, L., Iglesias-Pedraz, J.M., Kircher, S., et al. (2008). Coordinated regulation of Arabidopsis thaliana development by light and gibberellins. Nature *451*, 475–479.

Fiorucci, A.-S., Galvão, V.C., Ince, Y.Ç., Boccaccini, A., Goyal, A., Allenbach Petrolati, L., Trevisan, M., and Fankhauser, C. (2020). PHYTOCHROME INTERACTING FACTOR 7 is important for early responses to elevated temperature in Arabidopsis seedlings. New Phytol. *226*, 50–58.

Franklin, K.A., Lee, S.H., Patel, D., Kumar, S.V., Spartz, A.K., Gu, C., Ye, S., Yu, P., Breen, G., Cohen, J.D., et al. (2011). PHYTOCHROME-INTERACTING FACTOR 4 (PIF4) regulates auxin biosynthesis at high temperature. Proc. Natl. Acad. Sci. USA *108*, 20231–20235.

Fu, X., and Harberd, N.P. (2003). Auxin promotes Arabidopsis root growth by modulating gibberellin response. Nature *421*, 740–743.

Fujioka, S., Li, J., Choi, Y.-H., Seto, H., Takatsuto, S., Noguchi, T., Watanabe, T., Kuriyama, H., Yokota, T., Chory, J., et al. (1997). The Arabidopsis deetiolated 2 mutant is blocked early in brassinosteroid biosynthesis. Plant Cell *9*, 1951–1962.

Gallego-Bartolomé, J., Minguet, E.G., Grau-Enguix, F., Abbas, M., Locascio, A., Thomas, S.G., Alabadí, D., and Blázquez, M.A. (2012). Molecular mechanism for the interaction between gibberellin and brassinosteroid signaling pathways in Arabidopsis. Proc. Natl. Acad. Sci. USA *109*, 13446–13451.

Gendreau, E., Traas, J., Desnos, T., Grandjean, O., Caboche, M., and Höfte, H. (1997). Cellular basis of hypocotyl growth in Arabidopsis thaliana. Plant Physiol. *114*, 295–305.

Gendron, J.M., Liu, J.S., Fan, M., Bai, M.Y., Wenkel, S., Springer, P.S., Barton, M.K., and Wang, Z.Y. (2012). Brassinosteroids regulate organ boundary formation in the shoot apical meristem of Arabidopsis. Proc. Natl. Acad. Sci. USA *109*, 21152–21157.

Guo, H., Duong, H., Ma, N., and Lin, C. (1999). The Arabidopsis blue-light receptor cryptochrome 2 is a nuclear protein regulated by a blue-light dependent post-transcriptional mechanism. Plant J. *19*, 279–287.

Hahm, J., Kim, K., Qiu, Y., and Chen, M. (2020). Increasing ambient temperature progressively disassemble Arabidopsis phytochrome B from individual photobodies with distinct thermostabilities. Nat. Commun. *11*, 1.

Hayes, S., Pantazopoulou, C.K., van Gelderen, K., Reinen, E., Tween, A.L., Sharma, A., de Vries, M., Prat, S., Schuurink, R.C., Testerink, C., et al. (2019). Soil salinity limits plant shade avoidance. Curr. Biol. *29*, 1669–1676.e4.

He, J.-X., Gendron, J.M., Sun, Y., Gampala, S.S.L., Gendron, N., Sun, C.Q., and Wang, Z.-Y. (2005). BZR1 is a transcriptional repressor with dual roles in brassinosteroid homeostasis and growth responses. Science *307*, 1634–1638.

Heisler, M.G., Ohno, C., Das, P., Sieber, P., Reddy, G.V., Long, J.A., and Meyerowitz, E.M. (2005). Patterns of auxin transport and gene expression during primordium development revealed by live imaging of the Arabidopsis inflorescence meristem. Curr. Biol. *15*, 1899–1911.

Hornitschek, P., Kohnen, M.V., Lorrain, S., Rougemont, J., Ljung, K., López-Vidriero, I., Franco-Zorrilla, J.M., Solano, R., Trevisan, M., Pradervand, S., et al. (2012). Phytochrome interacting factors 4 and 5 control seedling growth in changing light conditions by directly controlling auxin signaling. Plant J. *71*, 699–711.

Huang, X., Zhang, Q., Jiang, Y., Yang, C., Wang, Q., and Li, L. (2018). Shade-induced nuclear localization of PIF7 is regulated by phosphorylation and 14-3-3 proteins in Arabidopsis. eLife *7*, e31636.

Huq, E., and Quail, P.H. (2002). PIF4, a phytochrome-interacting bHLH factor, functions as a negative regulator of phytochrome B signaling in Arabidopsis. EMBO J. *21*, 2441–2450.

Ibañes, M., Fàbregas, N., Chory, J., and Caño-Delgado, A.I. (2009). Brassinosteroid signaling and auxin transport are required to establish the periodic pattern of Arabidopsis shoot vascular bundles. Proc. Natl. Acad. Sci. USA *106*, 13630–13635.

Ibañez, C., Delker, C., Martinez, C., Bürstenbinder, K., Janitza, P., Lippmann, R., Ludwig, W., Sun, H., James, G.V., Klecker, M., et al. (2018). Brassinosteroids dominate hormonal regulation of plant thermomorphogenesis via BZR1. Curr. Biol. *28*, 303–310.e3.

Jeong, Y.J., Corvalán, C., Kwon, S.Il., and Choe, S. (2015). Analysis of anti-BZR1 antibody reveals the roles BES1 in maintaining the BZR1 levels in Arabidopsis. J. Plant Biol. *58*, 87–95.

Josse, E.-M., Gan, Y., Bou-Torrent, J., Stewart, K.L., Gilday, A.D., Jeffree, C.E., Vaistij, F.E., Martínez-García, J.F., Nagy, F., Graham, I.A., et al. (2011). A DELLA in disguise: SPATULA restrains the growth of the developing Arabidopsis seedling. Plant Cell *23*, 1337–1351.

Jung, J.H., Domijan, M., Klose, C., Biswas, S., Ezer, D., Gao, M., Khattak, A.K., Box, M.S., Charoensawan, V., Cortijo, S., et al. (2016). Phytochromes function as thermosensors in Arabidopsis. Science *354*, 886–889.

Kim, B., Jeong, Y.J., Corvalán, C., Fujioka, S., Cho, S., Park, T., and Choe, S. (2014). Darkness and gulliver2/phyB mutation decrease the abundance of phosphorylated BZR1 to activate brassinosteroid signaling in Arabidopsis. Plant J. *77*, 737–747.

Koini, M.A., Alvey, L., Allen, T., Tilley, C.A., Harberd, N.P., Whitelam, G.C., and Franklin, K.A. (2009). High temperature-mediated adaptations in plant architecture require the bHLH transcription factor PIF4. Curr. Biol. *19*, 408–413.

Kozuka, T., Kobayashi, J., Horiguchi, G., Demura, T., Sakakibara, H., Tsukaya, H., and Nagatani, A. (2010). Involvement of auxin and brassinosteroid in the regulation of petiole elongation under the shade. Plant Physiol. *153*, 1608–1618.

Kurepin, L.V., Joo, S.H., Kim, S.K., Pharis, R.P., and Back, T.G. (2012). Interaction of brassinosteroids with light quality and plant hormones in regulating shoot growth of young sunflower and Arabidopsis seedlings. J. Plant Growth Regul. *31*, 156–164.

Lachowiec, J., Mason, G.A., Schultz, K., and Queitsch, C. (2018). Redundancy, feedback, and robustness in the Arabidopsis thaliana BZR/BEH gene family. Front. Genet. *9*, 523.

Lau, O.S., and Deng, X.W. (2012). The photomorphogenic repressors COP1 and DET1: 20 years later. Trends Plant Sci. *17*, 584–593.

Legris, M., Klose, C., Burgie, E.S., Rojas, C.C., Neme, M., Hiltbrunner, A., Wigge, P.A., Schäfer, E., Vierstra, R.D., and Casal, J.J. (2016). Phytochrome B integrates light and temperature signals in Arabidopsis. Science *354*, 897–900.

Legris, M., Nieto, C., Sellaro, R., Prat, S., and Casal, J.J. (2017). Perception and signalling of light and temperature cues in plants. Plant J. *90*, 683–697.

Lewis, D.R., Wu, G., Ljung, K., and Spalding, E.P. (2009). Auxin transport into cotyledons and cotyledon growth depend similarly on the ABCB19 multidrug resistance-like transporter. Plant J. *60*, 91–101.

Li, L., Ljung, K., Breton, G., Schmitz, R.J., Pruneda-Paz, J., Cowing-Zitron, C., Cole, B.J., Ivans, L.J., Pedmale, U.V., Jung, H.S., et al. (2012). Linking photoreceptor excitation to changes in plant architecture. Genes Dev. *26*, 785–790.

Ling, J.-J., Li, J., Zhu, D., and Deng, X.W. (2017). Noncanonical role of Arabidopsis COP1/SPA complex in repressing BIN2-mediated PIF3 phosphorylation and degradation in darkness. Proc. Natl. Acad. Sci. USA *114*, 3539–3544.

Lorrain, S., Allen, T., Duek, P.D., Whitelam, G.C., and Fankhauser, C. (2008). Phytochrome-mediated inhibition of shade avoidance involves degradation of growth-promoting bHLH transcription factors. Plant J. *53*, 312–323.

Luccioni, L.G., Oliverio, K.A., Yanovsky, M.J., Boccalandro, H.E., and Casal, J.J. (2002). Brassinosteroid mutants uncover fine tuning of phytochrome signaling. Plant Physiol. *128*, 173–181.

Ma, D., Li, X., Guo, Y., Chu, J., Fang, S., Yan, C., Noel, J.P., and Liu, H. (2016). Cryptochrome 1 interacts with PIF4 to regulate high temperature-mediated hypocotyl elongation in response to blue light. Proc. Natl. Acad. Sci. USA *113*, 224–229.

Martins, S., Montiel-Jorda, A., Cayrel, A., Huguet, S., Le Roux, C.P., Ljung, K., and Vert, G. (2017). Brassinosteroid signaling-dependent root responses to prolonged elevated ambient temperature. Nat. Commun. *8*, 309.

McNellis, T.W., von Arnim, A.G., Araki, T., Komeda, Y., Miséra, S., and Deng, X.-W. (1994). Genetic and molecular analysis of an allelic series of cop1 mutants suggests functional roles for the multiple protein domains. Plant Cell *6*, 487–500.

Michaud, O., Fiorucci, A.S., Xenarios, I., and Fankhauser, C. (2017). Local auxin production underlies a spatially restricted neighbor-detection response in Arabidopsis. Proc. Natl. Acad. Sci. USA *114*, 7444–7449.

Müller, K., Engesser, R., Schulz, S., Steinberg, T., Tomakidi, P., Weber, C.C., Ulm, R., Timmer, J., Zurbriggen, M.D., and Weber, W. (2013). Multi-chromatic control of mammalian gene expression and signaling. Nucleic Acids Res. *41*, e124.

Müller, K., Zurbriggen, M.D., and Weber, W. (2014). Control of gene expression using a red- and far-red light-responsive bi-stable toggle switch. Nat. Protoc. *9*, 622–632.

Neff, M.M., and Van Volkenburgh, E. (1994). Light-stimulated cotyledon expansion in Arabidopsis seedlings. The role of phytochromeB. Plant Physiol. *104*, 1027–1032.

Noguchi, T., Fujioka, S., Choe, S., Takatsuto, S., Yoshida, S., Yuan, H., Feldmann, K.A., and Tax, F.E. (1999). Brassinosteroid-insensitive dwarf mutants of Arabidopsis accumulate brassinosteroids. Plant Physiol. *121*, 743–752.

Nolan, T.M., Brennan, B., Yang, M., Chen, J., Zhang, M., Li, Z., Wang, X., Bassham, D.C., Walley, J., and Yin, Y. (2017). Selective autophagy of BES1 mediated by DSK2 balances plant growth and survival. Dev. Cell *41*, 33–46.e7.

Nolan, T.M., Vukasinović, N., Liu, D., Russinova, E., and Yin, Y. (2020). Brassinosteroids: multidimensional regulators of plant growth, development, and stress responses. Plant Cell *32*, 295–318.

Oh, E., Zhu, J.-Y., Bai, M.-Y., Arenhart, R.A., Sun, Y., and Wang, Z.-Y. (2014). Cell elongation is regulated through a central circuit of interacting transcription factors in the Arabidopsis hypocotyl. eLife *3*, e03031.

Oh, E., Zhu, J.Y., and Wang, Z.Y. (2012). Interaction between BZR1 and PIF4 integrates brassinosteroid and environmental responses. Nat. Cell Biol. *14*, 802–809.

Oh, J., Park, E., Song, K., Bae, G., and Choi, G. (2020). PHYTOCHROME INTERACTING FACTOR8 inhibits phytochrome A-mediated far-red light responses in Arabidopsis. Plant Cell *32*, 186–205.

Ohnishi, T., Szatmari, A.M., Watanabe, B., Fujita, S., Bancos, S., Koncz, C., Lafos, M., Shibata, K., Yokota, T., Sakata, K., et al. (2006). C-23 hydroxylation by Arabidopsis CYP90C1 and CYP90D1 reveals a novel shortcut in brassinosteroid biosynthesis. Plant Cell *18*, 3275–3288.

Oravecz, A., Baumann, A., Máté, Z., Brzezinska, A., Molinier, J., Oakeley, E.J., Adám, E., Schäfer, E., Nagy, F., and Ulm, R. (2006). CONSTITUTIVELY PHOTOMORPHOGENIC1 is required for the UV-B response in Arabidopsis. Plant Cell *18*, 1975–1990.

Pacín, M., Semmoloni, M., Legris, M., Finlayson, S.A., and Casal, J.J. (2016). Convergence of CONSTITUTIVE PHOTOMORPHOGENESIS 1 and PHYTOCHROME INTERACTING FACTOR signalling during shade avoidance. New Phytol. *211*, 967–979.

Pantazopoulou, C.K., Bongers, F.J., Küpers, J.J., Reinen, E., Das, D., Evers, J.B., Anten, N.P.R., and Pierik, R. (2017). Neighbor detection at the leaf tip adaptively regulates upward leaf movement through spatial auxin dynamics. Proc. Natl. Acad. Sci. USA *114*, 7450–7455.

Park, E., Kim, Y., and Choi, G. (2018). Phytochrome B requires PIF degradation and sequestration to induce light responses across a wide range of light conditions. Plant Cell *30*, 1277–1292.

Park, Y.-J., Lee, H.-J., Ha, J.-H., Kim, J.Y., and Park, C.-M. (2017). COP1 conveys warm temperature information to hypocotyl thermomorphogenesis. New Phytol. *215*, 269–280.

Pedmale, U.V., Huang, S.C., Zander, M., Cole, B.J., Hetzel, J., Ljung, K., Reis, P.A.B., Sridevi, P., Nito, K., Nery, J.R., et al. (2016). Cryptochromes interact directly with PIFs to control plant growth in limiting blue light. Cell *164*, 233–245.

Pham, V.N., Kathare, P.K., and Huq, E. (2018a). Phytochromes and phytochrome interacting factors. Plant Physiol. *176*, 1025–1038.

Pham, V.N., Kathare, P.K., and Huq, E. (2018b). Dynamic regulation of PIF5 by COP1–SPA complex to optimize photomorphogenesis in Arabidopsis. Plant J. *96*, 260–273.

Ponnu, J., and Hoecker, U. (2021). Illuminating the COP1/SPA ubiquitin ligase: fresh insights Into its structure and functions During plant photomorphogenesis. Front. Plant Sci. *12*, 662793.

Procko, C., Burko, Y., Jaillais, Y., Ljung, K., Long, J.A., and Chory, J. (2016). The epidermis coordinates auxin-induced stem growth in response to shade. Genes Dev. *30*, 1529–1541.

Procko, C., Crenshaw, C.M., Ljung, K., Noel, J.P., and Chory, J. (2014). Cotyledon-generated auxin is required for shade-induced hypocotyl growth in Brassica rapa. Plant Physiol. *165*, 1285–1301.

Pucciariello, O., Legris, M., Costigliolo Rojas, C.C., Iglesias, M.J., Hernando, C.E., Dezar, C., Vazquez, M., Yanovsky, M.J., Finlayson, S.A., Prat, S., et al. (2018). Rewiring of auxin signaling under persistent shade. Proc. Natl. Acad. Sci. USA *115*, 5612–5617.

Purlyte, E., Dhekne, H.S., Sarhan, A.R., Gomez, R., Lis, P., Wightman, M., Martinez, T.N., Tonelli, F., Pfeffer, S.R., and Alessi, D.R. (2018). Rab29 activation of the Parkinson's disease-associated LRRK2 kinase. EMBO J. *37*, 1–18.

Quint, M., Delker, C., Franklin, K.A., Wigge, P.A., Halliday, K.J., and van Zanten, M. (2016). Molecular and genetic control of plant thermomorphogenesis. Nat. Plants *2*, 15190.

Reed, J.W., Nagpal, P., Poole, D.S., Furuya, M., and Chory, J. (1993). Mutations in the gene for the red/far-red light receptor phytochrome B alter cell elongation and physiological responses throughout Arabidopsis development. Plant Cell *5*, 147–157.

Rittenberg, D., and Foster, G.L. (1940). A new procedure for quantitative analysis by isotope dilution, with application to the determination of amino acids and fatty acids. J. Biol. Chem. *133*, 737–744.

Roig-Villanova, I., Bou, J., Sorin, C., Devlin, P.F., and Martinez-García, J.F. (2006). Identification of primary target genes of phytochrome signaling. Early transcriptional control during shade avoidance responses in Arabidopsis. Plant Physiol. *141*, 85–96.

Roig-Villanova, I., and Martínez-García, J.F. (2016). Plant responses to vegetation proximity: a whole life avoiding shade. Front. Plant Sci. *7*, 236.

Romanowski, A., Furniss, J.J., Hussain, E., and Halliday, K.J. (2021). Phytochrome regulates cellular response plasticity and the basic molecular machinery of leaf development. Plant Physiol. *186*, 1220–1239.

Saito, M., Kondo, Y., and Fukuda, H. (2018). BES1 and BZR1 redundantly promote phloem and xylem differentiation. Plant Cell Physiol. *59*, 590–600.

Sakuraba, Y., Jeong, J., Kang, M.Y., Kim, J., Paek, N.C., and Choi, G. (2014). Phytochrome-interacting transcription factors PIF4 and PIF5 induce leaf senescence in Arabidopsis. Nat. Commun. *5*, 4636.

Samodelov, S.L., Beyer, H.M., Guo, X., Augustin, M., Jia, K.P., Baz, L., Ebenhöh, O., Beyer, P., Weber, W., Al-Babili, S., et al. (2016). Strigoquant: A genetically encoded biosensor for quantifying strigolactone activity and specificity. Sci. Adv. *2*, e1601266.

Savaldi-Goldstein, S., Baiga, T.J., Pojer, F., Dabi, T., Butterfield, C., Parry, G., Santner, A., Dharmasiri, N., Tao, Y., Estelle, M., et al. (2008). New auxin analogs with growth-promoting effects in intact plants reveal a chemical strategy to improve hormone delivery. Proc. Natl. Acad. Sci. USA *105*, 15190–15195.

Savaldi-Goldstein, S., Peto, C., and Chory, J. (2007). The epidermis both drives and restricts plant shoot growth. Nature *446*, 199–202.

Sellaro, R., Hoecker, U., Yanovsky, M., Chory, J., and Casal, J.J. (2009). Synergism of red and blue light in the control of Arabidopsis gene expression and development. Curr. Biol. *19*, 1216–1220.

Sellaro, R., Smith, R.W., Legris, M., Fleck, C., and Casal, J.J. (2019). Phytochrome B dynamics departs from photoequilibrium in the field. Plant Cell Environ. *42*, 606–617.

Sheerin, D.J., Menon, C., zur Oven-Krockhaus, S., Enderle, B., Zhu, L., Johnen, P., Schleifenbaum, F., Stierhof, Y.-D., Huq, E., and Hiltbrunner, A. (2015). Light-activated Phytochrome A and B interact with members of the SPA family to promote photomorphogenesis in Arabidopsis by disrupting the COP1-SPA complex. Plant Cell *27*, 189–201.

Silverstone, A.L., Jung, H.-S., Dill, A., Kawaide, H., Kamiya, Y., and Sun, T.-P. (2001). Repressing a repressor: gibberellin-induced rapid reduction of the RGA protein in Arabidopsis. Plant Cell *13*, 1555–1566.

Sorin, C., Salla-Martret, M., Bou-Torrent, J., Roig-Villanova, I., and Martínez-García, J.F. (2009). ATHB4, a regulator of shade avoidance, modulates hormone response in Arabidopsis seedlings. Plant J. *59*, 266–277.

Staneloni, R.J., Rodriguez-Batiller, M.J., Legisa, D., Scarpin, M.R., Agalou, A., Cerdán, P.D., Meijer, A.H., Ouwerkerk, P.B.F., and Casal, J.J. (2009). Bell-like homeodomain selectively regulates the high-irradiance response of phytochrome A. Proc. Natl. Acad. Sci. USA *106*, 13624–13629.

Stavang, J.A., Gallego-Bartolomé, J., Gómez, M.D., Yoshida, S., Asami, T., Olsen, J.E., García-Martínez, J.L., Alabadí, D., and Blázquez, M.A. (2009). Hormonal regulation of temperature-induced growth in Arabidopsis. Plant J. *60*, 589–601.

Strader, L.C., Culler, A.H., Cohen, J.D., and Bartel, B. (2010). Conversion of endogenous indole-3-butyric acid to indole-3-acetic acid drives cell expansion in Arabidopsis seedlings. Plant Physiol. *153*, 1577–1586.

Sun, J., Qi, L., Li, Y., Chu, J., and Li, C. (2012). PIF4-mediated activation of YUCCA8 expression integrates temperature into the auxin pathway in regulating Arabidopsis hypocotyl growth. PLoS Genet. *8*, e1002594.

Sun, T.P. (2011). The molecular mechanism and evolution of the GA-GID1-DELLA signaling module in plants. Curr. Biol. *21*, R338–R345.

Tao, Y., Ferrer, J.L., Ljung, K., Pojer, F., Hong, F., Long, J.A., Li, L., Moreno, J.E., Bowman, M.E., Ivans, L.J., et al. (2008). Rapid synthesis of auxin via a new tryptophan-dependent pathway is required for shade avoidance in plants. Cell *133*, 164–176.

Tarkowská, D., Novák, O., Oklestkova, J., and Strnad, M. (2016). The determination of 22 natural brassinosteroids in a minute sample of plant tissue by UHPLC–ESI–MS/MS. Anal. Bioanal. Chem. *408*, 6799–6812.

Tsuge, T., Tsukaya, H., and Uchimiya, H. (1996). Two independent and polarized processes of cell elongation regulate leaf blade expansion in *Arabidopsis thaliana* (L) Heynh. Development *122*, 1589–1600.

Tsukaya, H., Tsuge, T., and Uchimiya, H. (1994). The cotyledon: A superior system for studies of leaf development. Planta *195*, 309–312.

Turk, E.M., Fujioka, S., Seto, H., Shimada, Y., Takatsuto, S., Yoshida, S., Wang, H., Torres, Q.I., Ward, J.M., Murthy, G., et al. (2005). BAS1 and SOB7 act redundantly to modulate Arabidopsis photomorphogenesis via unique brassinosteroid inactivation mechanisms. Plant J. *42*, 23–34.

Wang, Z.-Y., Nakano, T., Gendron, J., He, J., Chen, M., Vafeados, D., Yang, Y., Fujioka, S., Yoshida, S., Asami, T., et al. (2002). Nuclear-localized BZR1 mediates brassinosteroid-induced growth and feedback suppression of brassinosteroid biosynthesis. Dev. Cell *2*, 505–513.

Xu, W., Huang, J., Li, B., Li, J., and Wang, Y. (2008). Is kinase activity essential for biological functions of BRI1? Cell Res. *18*, 472–478.

Yang, M., Li, C., Cai, Z., Hu, Y., Nolan, T., Yu, F., Yin, Y., Xie, Q., Tang, G., and Wang, X. (2017). SINAT E3 ligases control the light-mediated stability of the brassinosteroid-activated transcription factor BES1 in Arabidopsis. Dev. Cell *41*, 47–58.e4.

Yin, Y., Wang, Z.Y., Mora-Garcia, S., Li, J., Yoshida, S., Asami, T., and Chory, J. (2002). BES1 accumulates in the nucleus in response to brassinosteroids to regulate gene expression and promote stem elongation. Cell *109*, 181–191.

Zhang, J., Stankey, R.J., and Vierstra, R.D. (2013). Structure-guided engineering of plant phytochrome B with altered photochemistry and light signaling. Plant Physiol. *161*, 1445–1457.

Please cite this article in press as: Costigliolo Rojas et al., Organ-specific COP1 control of BES1 stability adjusts plant growth patterns under shade or warmth, Developmental Cell (2022), https://doi.org/10.1016/j.devcel.2022.07.003



## STAR★METHODS

### KEY RESOURCES TABLE

| REAGENT or RESOURCE | SOURCE | IDENTIFIER |
|---|---|---|
| Antibodies | | |
| Rabbit polyclonal anti-BES1 | Yin et al., 2002 | N/A |
| Rabbit IgG (H+L) Secondary Antibody | Thermo Fisher | Cat# A24531; RRID: AB_2535999 |
| Anti Prx (2-Cys Peroxirredoxin) | S. Mora-Garcia (Instituto Leloir, Buenos Aires) | N/A |
| anti-HA-HRP | Roche | Cat# 3F10; RRID: AB_2610670 |
| anti-c-myc | Roche | Cat# 9E10; RRID: AB_2533008 |
| anti-GFP | Clontech | Cat# JL8; RRID: AB_2336883 |
| Chemicals, peptides, and recombinant proteins | | |
| MG132 | MERCK | 1211877-36-9 |
| E64 | MERCK | 66701-25-5 |
| CHX | MERCK | 66-81-9 |
| Picloram | TORDON | 24K |
| GA4 | MERCK | 468-44-0 |
| Brassinazole | MERCK | 280129-83-1 |
| Epibrassinolide | MERCK | 78821-43-9 |
| Paclobutrazol | MERCK | 76738-62-0 |
| Experimental models: organisms/strains | | |
| *Arabidopsis thaliana: bes1-1* | He et al., 2005 | SALK_098634 |
| *Arabidopsis thaliana: bes1-1 bzr1-2* | Saito et al., 2018 | N/A |
| *Arabidopsis thaliana: bes1-D* | Ibañes et al., 2009 | N/A |
| *Arabidopsis thaliana: bes1-2* | Lachowiec et al., 2018 | WiscDsLox246D02 |
| *Arabidopsis thaliana: bri1-301* | Xu et al., 2008 | N/A |
| *Arabidopsis thaliana: bri1-5* | Noguchi et al., 1999 | N/A |
| *Arabidopsis thaliana: bzr1-1* | Saito et al., 2018 | N/A |
| *Arabidopsis thaliana: bzr1-1D* | Wang et al., 2002 | N/A |
| *Arabidopsis thaliana*: Col-0 | N/A | N/A |
| *Arabidopsis thaliana: cop1-4* | McNellis et al., 1994 | N/A |
| *Arabidopsis thaliana: cry1-301* | Guo et al., 1999 | N/A |
| *Arabidopsis thaliana: det2-1* | Chory et al., 1991 | N/A |
| *Arabidopsis thaliana: ga1-3 rgl2-1 gai-t6 rga-t2 (dellaq)* | Achard et al., 2006 | N/A |
| *Arabidopsis thaliana*: Landsberg *erecta* | N/A | N/A |
| *Arabidopsis thaliana: phyB-9* | Reed et al., 1993 | N/A |
| *Arabidopsis thaliana: pif4-101* | Lorrain et al., 2008 | N/A |
| *Arabidopsis thaliana: pif4-101 pif5 (pil6-1) pif7-1* | de Wit et al., 2015 | N/A |
| *Arabidopsis thaliana: rot3-1* | Tsuge et al., 1996 | N/A |
| *Arabidopsis thaliana: sav3-1* | Tao et al., 2008 | N/A |
| *Arabidopsis thaliana*: Wassilewskija | N/A | N/A |
| *Arabidopsis thaliana: yuccaq* | Tao et al., 2008 | N/A |
| *Arabidopsis thaliana: p35S:bes1-D -GFP* | Espinosa-Ruiz et al., 2017 | N/A |
| *Arabidopsis thaliana: p35S:BES1-GFP* | This paper | N/A |
| *Arabidopsis thaliana: p35S:BES1-GFP bri-301* | This paper | N/A |

(*Continued on next page*)

Please cite this article in press as: Costigliolo Rojas et al., Organ-specific COP1 control of BES1 stability adjusts plant growth patterns under shade or warmth, Developmental Cell (2022), https://doi.org/10.1016/j.devcel.2022.07.003





*Continued*

| REAGENT or RESOURCE | SOURCE | IDENTIFIER |
|---|---|---|
| *Arabidopsis thaliana: p35S:BZR1-YFP bri-301* | This paper | N/A |
| *Arabidopsis thaliana: p35S:COP1-YFP* | Oravecz et al., 2006 | N/A |
| *Arabidopsis thaliana: p35S:DWF4 (DWF4-OX)* | Choe et al., 2001 | N/A |
| *Arabidopsis thaliana: PIF4 OX-MYC* | Sakuraba et al., 2014 | N/A |
| *Arabidopsis thaliana: pBES1:BES1-GFP* | Yin et al., 2002 | N/A |
| *Arabidopsis thaliana: pBES1:BES1-GFP in cop1-4* | This paper | N/A |
| *Arabidopsis thaliana: pBES1:BES1-GFP in phyB-9* | This paper | N/A |
| *Arabidopsis thaliana: pBES1:BES1-GFP in pif4-101* | This paper | N/A |
| *Arabidopsis thaliana: pBES1:BES1-GFP pCOP1:COP1-mCHERRY* hemizygous | This paper | N/A |
| *Arabidopsis thaliana: pBZR1:BZR11-GFP* | Gendron et al., 2012 | N/A |
| *Arabidopsis thaliana: pDR5rev:3XVENUS-N7* | Heisler et al., 2005 | N/A |
| *Arabidopsis thaliana: phyB-9 pUBQ10-YFP* | Zhang et al., 2013 | N/A |
| *Arabidopsis thaliana: pPIF4:PIF4-GFP* | Pucciariello et al., 2018 | N/A |
| *Arabidopsis thaliana: pRGA:RGA-GFP* | Fu and Harberd, 2003 | N/A |
| *Brassica napus cv Hyola 61* | J. Botto (IFEVA, Buenos Aires) | N/A |
| Experimental models: Cell lines | | |
| Hamster: CHO cells | M. Zurbriggen (Dusseldorf University) | N/A |
| Recombinant DNA | | |
| *pBES1-pCMVmin::FLUC::tNos* | M. Zurbriggen (Dusseldorf University) | N/A |
| *pBES1(short)-pCMVmin::FLUC::tNos* | M. Zurbriggen (Dusseldorf University) | N/A |
| *pSV40::PIF4-VP16::pA* | M. Zurbriggen (Dusseldorf University) | N/A |
| *pSV40::BFP::pA* | M. Zurbriggen (Dusseldorf University) | N/A |
| *pSV40::NanoLUC::pA* | M. Zurbriggen (Dusseldorf University) | N/A |
| *pBES1-pCMVmin-Fluc* | M. Zurbriggen (Dusseldorf University) | N/A |
| *pBES1(short)-pCMVmin-Fluc* | M. Zurbriggen (Dusseldorf University) | N/A |
| *p35s-PIF4-pNos* | M. Zurbriggen (Dusseldorf University) | N/A |
| *p35s-RENLuc-pNos* | M. Zurbriggen (Dusseldorf University) | N/A |
| *p35s-eGFP-pNos (Stuffer)* | M. Zurbriggen (Dusseldorf University) | N/A |
| Oligonucleotides (Table S1) | | |
| Software and algorithms | | |
| Image J | NHI | https://imagej.nih.gov/ij/ |
| Graph Pad Prism | GraphPad Software | https://www.graphpad.com/ |
| Infostat | FCA-UNC | https://www.infostat.com.ar/ |

## RESOURCE AVAILABILITY

### Lead contact

Lead contact, Professor Jorge Casal (casal@ifeva.edu.ar).

### Materials availability

Further information and requests for resources and reagents should be directed to and will be fulfilled by the lead contact.

### Data and code availability

- This paper does not analyse existing, publicly available data.

- This paper does not report original code.
- Any additional information required to reanalyse the data reported in this paper is available from the lead contact upon request.

## EXPERIMENTAL MODEL AND SUBJECT DETAILS

### Plant Material

The genotypes of *Arabidopsis* (*Arabidopsis thaliana*) or *Brassica napus* are listed in the key resources table. The wild type (WT) was Col-0, expect for the experiments with *dellaq* (Landsberg *erecta*) or *bri1-5* (Wassilewskija).

We introgressed the *pBES1: BES1-GFP* transgene into the *cop1-4*, *pif4-101*, and *phyB-9* background by genetic crosses. The resulting F2 seeds were sown on 1% agar containing MS and 50 mg/ml kanamycin to select for the presence of the transgene, which provides resistance to this antibiotic. Homozygous lines were selected in the F3 generation either by phenotype (*cop1-4* and *phyB-9*) or by using specific primers (*pif4-101*).

The lines 355S*:BES1-GFP bri-301* and *35S.BZR1-GFP bri1-301* were generated by transforming *bri1-301* mutant plants via *Agrobacterium tumefaciens* by the flower dipping method using *pEarleyGate103:AtBES1* and *pEarleyGate103:AtBZR1*. T1 plants were selected on soil by spraying with a Basta solution. Subsequent rounds of selection were performed on MS plates with the addition of 15 mg/ml phosphinothricin (Duchefa). For the selection of single-insertion lines, T2 seeds from individual T1 transgenic lines were plated regularly onto MS plates containing phosphinothricin, and the ratio of resistant to sensitive plants was scored 12 days later. Only lines that showed a ratio close to 3 resistant to 1 sensitive were kept for further analysis, and transferred to soil. T3 seeds were scored under the same conditions to select homozygous, non-segregating lines for the transgenes.

The hemizygous *pBES1:BES1-GFP pCOP1:COP1-mCHERRY* is the F1 generation of crosses between the homozygous lines. The homozygous *pCOP1:COP1-mCHERRY* line was kindly provided by Professor Andreas Hiltbrunner (Institute of Biology II, Department of Molecular Plant Physiology, Faculty of Biology, University of Freiburg, Germany) and will be described in detail elsewhere.

## METHOD DETAILS

### Growth conditions and treatments

Seeds were sown on 10 ml of 1% agar in clear plastic boxes (5 × 8 × 2 $cm^3$). The boxes were incubated in darkness at 5°C for 3 d. Then, the seedlings were grown under white-light photoperiods (10 h) provided by a mixture of fluorescent and halogen lamps providing 90-100 μmol $m^{-2}$ $s^{-1}$ of photosynthetically active radiation and a red / far-red ratio= 1.1 at 20°C. One hour after the beginning of the photoperiod of day 4, we transferred the seedlings to the shade or warmth treatments, whilst the controls remained under white light at 20°C. Shade was simulated by using the same light sources described for control conditions in combination with two green acetate filters (no. 089; LEE Filters, Hampshire, UK) to reduce photosynthetically active radiation to 10 μmol $m^{-2}$ $s^{-1}$ and the red / far-red ratio to 0.1 (Pacín et al., 2016). Warm conditions were 90-100 μmol $m^{-2}$ $s^{-1}$ of photosynthetically active radiation and a red / far-red ratio= 1.1 at 28°C.

### Hypocotyl and cotyledon growth rate

Fifteen seeds per genotype were sown in each replicate box. The plates were placed vertically for the hypocotyl growth experiments and horizontally for cotyledon growth experiments. The seedlings were photographed using a digital camera (PowerShot; Canon, Tokyo, Japan) 1 and 10 h after the beginning of day 4 (0 h and 9 h after the beginning of treatments). Hypocotyl length or cotyledon area was determined at both time points with image processing software (Sellaro et al., 2009) and used to calculate the increments over the 9-h treatment period.

### Confocal microscopy

Confocal fluorescence images were taken with an LSM5 Pascal (Zeiss) laser scanning microscope with a Plan-Apochromat 40×/1.2 objective lens. For chloroplast visualization, probes were excited with a He-Ne laser (λ = 543 nm) and fluorescence was detected using an LP560 filter. For visualization of GFP/YFP fusion proteins and VENUS, probes were excited with an Argon laser (λ = 488 nm) and fluorescence was detected using BP 505-530 and BP 505-570 filters, respectively. For hypocotyl observations, the pinhole was closed to obtain a 5 μm optical sectioning. For cotyledon observations, the pinhole was closed to obtain a 2 μm optical sectioning. In all cases the images were taken from the epidermis (although this may include the first sub-epidermal layer). Confocal fluorescence images were taken 4 h or 8 h after the application of shade or warmth treatments. We measured the fluorescence of all the nuclei in each image (we show representative images). We then divided the sum of these fluorescence values by the number of cells in the image. Therefore, the nuclei with no detectable fluorescence did not contribute to the numerator of the equation but their cells were included in the denominator. To calculate the number of cells we measured the area of five cells and divided the area of the image by the average area of a cell.

### Pharmacological treatments

Where indicated, 100 μM MG132, 30 μM E64, 100 μM Cycloheximide, 0.1; 1; 5 or 10 μM Picloram, 5 μM Paclobutrazol, 3 μM GA4 or 10 nM epibrassinolide were added, 3 h before starting the shade or warmth treatments, whereas 1; 5; or 10 μM Brassinazole were

added 14 h before starting the treatments. Confocal fluorescence images of *pBES1:BES1-GFP, pRGA:RGA-GFP* and *DR5-VENUS* were taken 4 h after the beginning of shade or warmth and growth measurements between 0 and 9 h after the beginning of treatments.

### Protein blots

We separately collected samples of cotyledons and samples of hypocotyls from *B. napus* and samples of cotyledons of *A. thaliana*, or harvested whole seedlings of *A. thaliana*. Harvest was at the end of the photoperiod when we applied shade or warmth treatments. Samples were ground in liquid nitrogen until a fine powder was obtained. Then, total protein was extracted with 100 μl of 2X loading buffer (125 mM Tris / HCl [pH 7.4], 2% SDS, 10% glycerol, 6 M urea), 1% β-mercaptoethanol and 1% PMSF). The samples were heated 3 min at 95°C and centrifuged 20 min at 13,000 rpm (4°C). Proteins were separated by electrophoresis on 10% Acrylamide / Bisacrylamide gels. A native antibody against the BES1 protein (Yin et al., 2002) was used as primary antibody. Anti-rabbit-HRP was used as a secondary antibody. The Amersham ECL Prime Western Blotting Detection Reagent Kit (GE Healthcare, Little Chalfont, UK) and ImageQuant ™ LAS 4000 (GE Healthcare) were used for detection. We used Ponceau red staining (*A. thaliana*) or the band produced by an antibody that recognizes 2-Cys Peroxirredoxin (Prx) of chloroplasts (*B. napus*) as controls of uniform loading. For band quantification we used ImageJ. The intensity of each band was divided by the intensity of its respective load control.

### Quantitative reverse transcriptase-PCR

Samples were harvested in liquid Nitrogen 4 h after the beginning of day 4 (i.e., after 3 h of shade or warmth treatments). Total RNA was extracted with Spectrum Plant Total RNA Kit (Sigma-Aldrich) and subjected to a DNAse treatment with RQ1 RNase-Free DNase (Promega). cDNA derived from this RNA was synthesized using Invitrogen SuperScript II and an oligo-dT primer. The synthesized cDNAs were amplified with FastStart Universal SYBRGreen Master (Roche) using the 7500 Real Time PCR System (Applied Biosystems, available from Invitrogen) cycler. The *UBIQUITIN-CONJUGATING ENZYME 2* (*UBC2*) gene was used as the normalization control (Staneloni et al., 2009).

### Brassinosteroid analysis

The cotyledons and hypocotyls were separately harvested from plants from *A. thaliana* and *B. napus*, 5 h after the beginning of day 4 (i.e., after 4 h of shade or warmth treatment). Samples were analyzed for brassinosteroid content according to the method described (Tarkowská et al., 2016). Briefly, freeze-dried samples of 5-25 mg were homogenized to a fine consistency using 2.8-mm zirconium oxide beads (Retsch GmbH & Co. KG, Haan, Germany) and a MM 400 vibration mill (Retsch GmbH & Co. KG, Haan, Germany) at a frequency of 27 Hz for 3 min. The samples were then extracted overnight with stirring at 4 °C using a benchtop laboratory rotator Stuart SB3 (Bibby Scientific Ltd., Staffordshire, UK) after adding with 1 mL ice-cold 60 % acetonitrile and mixture of [$^2H_3$]brassinolide, [$^2H_3$]castasterone, [$^2H_3$]24-epibrassinolide, [$^2H_3$]24-epicastasterone, [$^2H_3$]28-norbrassinolide, [$^2H_3$]28-norcastasterone and [$^2H_3$]typhasterol as stable isotope labelled internal standards (OlChemIm Ltd., Olomouc, Czech Republic). The samples were further centrifuged, purified on polyamide SPE columns (Supelco, Bellefonte, PA, USA) and then analysed by UHPLC-MS/MS (Micromass, Manchester, UK). The data were analysed by using Masslynx 4.2 software (Waters, Milford, MA, USA) and BRs content was finally quantified by the standard isotope-dilution method (Rittenberg and Foster, 1940).

### Chromatin immunoprecipitation (ChIP)

For ChIP assays, seedlings were grown on MS-sucrose-agar plates (half-strength Murashige & Skoog, 0.05% MES, 1% sucrose, 0.8% phyto agar, pH 5.7) at 22°C under light with a high red / far-red ratio (blue, 20 μmol·m–2·s–1; red, 20 μmol·$m^{-2}$·$s^{-1}$; far-red, 10 μmol·$m^{-2}$·$s^{-1}$) for 4 d, then either maintained under light with high red / far-red ratio or transferred to light with low red / far-red ratio light (blue, 2 μmol·$m^{-2}$·$s^{-1}$; red, 2 μmol·$m^{-2}$·$s^{-1}$; far-red, 10 μmol·$m^{-2}$·$s^{-1}$) for 4 h. ChIP experiments were performed as previously described (Oh et al., 2020).

### One-hybrid in mammalian cells

Chinese Hamster ovary (CHO-K1) cells were cultivated in HAM's F12 medium with 10% (v/v) fetal bovine serum (FBS) and 1% (v/v) Penicillin/Streptomycin.

24 h before transfection 50,000 cells in 500 μl medium were seeded per well in 24-well plates (Corning). 1,25 μg DNA per well were diluted in 50 μl of OptiMEM and mixed with a PEI/OptiMEM mix [2.5 μL PEI solution (1 mg/ml) in 50 μL OptiMEM] (Blomeier et al., 2021). The ratio between target plasmid (pBES1-pCMVmin::FLUC::tNos) and inducer plasmid (pSV40::PIF4-VP16::pA) was 1:4 (additionally 0,1 μg of normalization plasmid). 100 μl of transfection mix was added to each well in a drop-wise manner. Medium was exchanged after 4 h. 24 h post transfection luminescence was measured with a Berthold Technologies Centro $XS^3$ LB 960 Microplate luminometer for FLUC and NanoLuc (normalization) (Blomeier et al., 2021). Cells were lysed with 250 μl lysis buffer and 1mM 1,4-Dithiothreitol (DTT) on ice, and afterwards carefully resuspended as previously described (Baaske et al., 2018). 80 μl of cell lysate was transferred into 96-well white plates. Right before measurement, 20 μl of firefly substrate [0.47 mM D-luciferin (Biosynth AG), 20 mM tricine, 2.67 mM $MgSO_4 \cdot 7H_2O$, 0.1 mM EDTA·$2H_2O$, 33.3 mM dithiothreitol, 0.52 mM adenosine 5′-triphosphate, 0.27 mM acetyl–coenzyme A, 5 mM NaOH, 0.26 mM $MgCO_3 \cdot 5H_2O$, in $H_2O$] or coelenterazine (472 mM coelenterazine stock solution in methanol, diluted directly before use 1:15 in phosphate-buffered saline for NanoLuc determination, were added to the samples.

### Protoplast transactivation

Protoplasts were isolated from 2-week old *A. thaliana* seedlings grown in 12-cm square plates containing SCA medium (0.32 % (wt/vol) Gamborg's B5 basal salt powder with vitamins (bioWORLD), 4 mM $MgSO_4 \cdot 7H_2O$, 43.8 mM sucrose and 0.8% (wt/vol) phytoagar in $H_2O$, pH 5.8, autoclaved, 0.1% (vol/vol) Gamborg's B5 Vitamin Mix (bioWORLD), with a 22 °C, 16-h light – 8-h dark cycle (Samodelov et al., 2016). The leaf material was carefully sliced with a scalpel and incubated in darkness at 23 °C overnight in MMC solution (10 mM MES, 40 mM $CaCl_2 \cdot H_2O$, 467 mM mannitol, pH 5.8, sterile filtered) containing 0.5% cellulase Onozuka R10 and macerozyme R10 (SERVA Electrophoresis). After ~18h, the lysate was thoroughly and carefully mixed, passed through a 70 μm pore size sieve and transferred to a MSC solution (10 mM MES, 0.4 M sucrose, 20 mM $MgCl_2 \cdot 6H_2O$, 467 mM mannitol, pH 5.8, sterile filtered) and overlaid with MMM solution (15 mM $MgCl_2$, 5 mM MES, 467 mM mannitol, pH 5.8, sterile filtered). After centrifugation the protoplasts were collected at the interphase and transferred to a W5 solution (2 mM MES, 154 mM NaCl, 125 mM $CaCl_2 \cdot 2H_2O$, 5 mM KCl, 5 mM glucose, pH 5.8, sterile filtered) and counted in a Rosenthal chamber and subsequently diluted to 500,000 protoplasts per 100 μl. The plasmids were transferred by polyethylene-glycol-mediated transformation. Mixtures of the different plasmids to a final amount of 30 μg DNA were used to transform 500,000 protoplasts in non-treated 6-well plates by dropwise addition of a PEG solution (4 g PEG4000, 2.5 ml of 800 mM mannitol, 1 ml of 1 M $CaCl_2$ and 3 ml $H_2O$). After 8-min incubation, 120 μl MMM and 1,240 μl PCA (0.32% (wt/vol) Gamborg's B5 basal salt powder with vitamins (bioWorld), 2 mM $MgSO_4 \cdot 7H_2O$, 3.4 mM $CaCl_2 \cdot 2H_2O$, 5 mM MES, 0.342 mM l-glutamine, 58.4 mM sucrose, 444 mM glucose, 8.4 μM calcium pantothenate, 2% (vol/vol) biotin from a biotin solution 0.02% (wt/vol) 0.1% (vol/vol) in H2O, pH 5.8, sterile filtered, 0.1% (vol/ vol) Gamborg's B5 Vitamin Mix, 64.52 μg $\mu l^{-1}$ ampicillin, were added to get a final volume of 1.6 ml protoplast suspension. The protoplasts were kept in darkness for ~24 h at 22°C.

Four technical replicates of 80 μl protoplast suspensions (approximately 25,000 protoplasts) were pipetted into two separate 96-well white flat-bottom plates (Costar) for parallel determination of activity of both luciferases. Addition of 20 μl of either FLuc substrate (0.47 mM d-luciferin (Biosynth AG), 20 mM tricine, 2.67 mM $MgSO_4 \cdot 7H_2O$, 0.1 mM EDTA·$2H_2O$, 33.3 mM dithiothreitol, 0.52 mM adenosine 5′-triphosphate, 0.27 mM acetyl– coenzyme A, 5 mM NaOH, 264 μM $MgCO_3 \cdot 5H_2O$, in $H_2O$, pH 8) or RLuc substrate (0.472 mM coelenterazine stock solution in methanol, diluted directly before use, 1:15 in PBS) was performed prior to luminescence determination in a plate reader (determination of 20-min kinetics, integration time 0.1 s).

### Co-immunoprecipitation

The constructs that express *DsRED-COP1-HA* and *c-myc-SPA1* have been described (Blanco-Touriñán et al., 2020). To prepare the *YFP-BES1* fusion under the control of the *35S* promoter, the *BES1 CDS* was transferred to the pEarleyGate104 vector (Earley et al., 2006) by LR. Constructs were used to transform *Agrobacterium tumefaciens* strain C58. Co-immunoprecipitation assays were carried out as described (Blanco-Touriñán et al., 2020), with minor modifications. Different mixtures of bacterial cultures, including bacteria expressing the silencing suppressor p19, were used to infiltrate leaves of 1-month-old *Nicotiana benthamiana* plants grown under long-day conditions (16 h light: 8 h dark). Samples were harvested at dawn three days after infiltration. One mL of ground, frozen tissue was homogenized in 700 μL of extraction buffer (25 mM Tris-HCl pH 7.5, 10% glycerol, 1 mM EDTA pH 8.0, 150 mM NaCl, and 1x protease inhibitor cocktail [cOmplete, EDTA-free; Roche]). Extracts were kept on ice for 20 min before cell debris were removed by centrifugation at maximum speed in a benchtop centrifuge at 4°C twice. Sixty μg of total proteins were denatured in Laemmli buffer and set aside to be used as input. One mg of total protein in 1 mL of extraction buffer were incubated with 25 μL of anti-GFP-coated paramagnetic beads (Miltenyi) at 4 ºC for 2 h in a rotating wheel. Extracts were loaded into μColumns (Miltenyi) at room temperature. Columns were washed four times with 200 μL of cold extraction buffer and proteins were eluted under denaturing conditions in 70 μL of elution buffer (Miltenyi). Sixty-three μL of the immunoprecipitated samples (90%) were run in a 12% SDS-PAGE along with 30 μg of input. Proteins were transferred to a PVDF membrane and sequentially immunodetected with an anti-HA-HRP antibody (3F10, 1:5000; Roche) and, after strip-out, with an anti-c-myc antibody (9E10, 1:1000; Roche). The remaining 7 μL of the IPs, along with 30 μg of input, were processed in the same way and the membrane probed with an anti-GFP antibody (JL8, 1:5000; Clontech). Chemiluminiscence was detected with SuperSignal™ West Femto (Thermo-Fisher Scientific) and imaged with the ImageQuant™ 800 biomolecular imager (Amersham).

### Bi-molecular fluorescence complementation

Leaves of one-month-old *N. benthamiana* plants grown under 16 h light:8 h dark photoperiods at 25°C were infiltrated with the different mixtures of *A. tumefaciens* C58 cells carrying the necessary vectors before imaging by confocal microscopy (Zeiss 780 Axio Observer) with a water-immersion objective lens (Capochromat 40X/1.2; Zeiss) the fourth day after infiltration. Samples were kept in darkness on the day of imaging. YFP was excited with an Argon laser (488 nm) and detected at 515-590 nm. Chloroplasts autofluorescence was detected between 650 and 760 nm.

### Co-localization assays in *N. benthamiana*

Leaves of one-month-old *N. benthamiana* plants grown under 16 h light/8 h dark photoperiod at 25 °C were infiltrated with the different mixtures of *A. tumefaciens* C58 cells carrying the necessary vectors and the p19 silencing suppressor before imaging by confocal microscopy (Zeiss 780 Axio Observer) with a water-immersion objective lens (Capochromat 40X/1.2; Zeiss) the fourth day after infiltration. Samples were kept in darkness on the day of imaging. YFP was excited with an Argon laser (488 nm) and

detected at 520-560 nm. DsRED was excited with a DPSS 561-10 laser (561 nm) and detected at 565-625 nm. YFP and DsRED signals were detected by independent tracks. Chloroplasts autofluorescence was detected between 660 and 760 nm.

### Protein-protein interaction assays in mammalian cells

Chinese hamster ovary cells (CHO-K1) (DSMZ, Braunschweig, Germany) were cultivated in HAM's F12 medium (PAN Biotech, Aidenbach, Germany) supplemented with 10% (v/v) tetracycline-free fetal bovine serum (PAN Biotech). For transfection, 50,000 cells per replicate were transfected with 0.75 μg of total DNA using polyethyleneimine (PEI; Polysciences Inc. Europe, Hirschberg, Germany), as described elsewhere (Müller et al., 2013). Medium was exchanged 4 h after transfection. Cells were transfected with reporter plasmid *tetO13-pCMVmin :: SEAP :: T BGH :: pSV40 :: Gaussia :: T SV40* (*pPF034*) and the different plasmid combinations, in equal amounts. 15 μM phycocyanobilin (24 mM stock solution in DMSO; Frontier Scientific, Logan, UT, USA) were added to the cells 24 h post transfection. After 1 h incubation, cells were illuminated with 20 μmol $m^{-2}$ $s^{-1}$ red light (660 nm, LED light boxes) for 24 h, or kept in darkness. As a negative control, one set up was transfected only with the reporter plasmid.

#### *SEAP activity assay*

The supernatant/medium of transfected cells was transferred to 96-well round bottom plates and incubated at 68°C for 1 h to inactivate endogenous phosphatases. 80 μl of each sample were transferred to 96-well flat-bottom plates containing 100 μl of SEAP buffer per well (20 mM homoarginine, 1 mM $MgCl_2$, 21% (v/v) diethanolamine). Right after addition of 20 μl 120 mM para-nitrophenyl phosphate, absorption at 405 nm was determined every minute for an hour using a BMG Labtech CLARIOstar (Berthold Technologies, Bad Wildbad, Germany) plate reader and used to calculate the activity (Blomeier et al., 2021).

For GAUSSIA luciferase assay, after illumination, 20 μl of supernatant were transferred to a 96-well white plate containing 60 μl of PBS (2.68 mM KCl, 1.47 mM $KH_2PO_4$, 8.03 mM $Na_2PO_4$, 137 mM NaCl). Right after addition of 20 μl coelenterazine (472 mM stock solution in methanol, diluted 1:1,500 in PBS; Carl Roth, Karlsruhe, Germany), bioluminescence was measured for 20 min using a LB 942 multimode plate reader (Baaske et al., 2018).

## QUANTIFICATION AND STATISTICAL ANALYSIS

The number of biological replicates is given in the legend of the figures. In confocal microscopy experiments and cotyledon or hypocotyl growth experiments, several seedlings grown within the same box were analysed. However, the data coming from these seedlings were pooled into one biological replicate. For this reason, we give the number of replicate boxes of seedlings. Data were analysed by using ANOVA and Bonferroni post-test (GraphPad Prism) taking into account the occurrence of multiple comparisons defined a priori.

Growth and confocal microscopy fluorescence data were normalised to the control condition by dividing the individual values by the average of the control (light, 20 °C) in the same experiment. This procedure increased accuracy by reducing the variability among experiments. In quantitative reverse transcriptase-PCR counts were divided by the of the reference gene in the same sample before normalisation to the control condition. Similarly, in protein blots band intensity was divided by the intensity of the loading control before normalisation to the control condition. Although for consistency we present protein blot data relative to the control condition, for statistics we re-analysed the data normalising to the average of the experiment to avoid heterogeneity of variance (since we had one control sample per experiment, the control normalised to itself gave null variance).

We used the step-wise model of multiple regression analysis (Infostat) to investigate whether the effects of phyB, COP1 and PIF4 on nuclear BES1 levels could be quantitatively accounted for their effects on *BES1* gene expression. We included phyB, COP1 and PIF4 activities and *BES1* expression levels as explanatory variables and nuclear BES1 as response variable. The variables PIF4 and phyB, originally included in the analysis, were excluded by the model (we set the stringency at $p < 0.01$ to include and retain a variable), indicating that the information that they provide is already contained in the information provided by *BES1* expression. Conversely, COP1 was retained (in addition to *BES1* mRNA) indicating that its effects cannot be accounted for by changes in *BES1* expression. The values of the explanatory variables were standardised to obtain coefficients of comparable magnitude.